

# Benchmarking the dynamic luminescent properties and UV stability of B<sub>18</sub>H<sub>22</sub>-based materials

Kierstyn P. Anderson,<sup>a</sup> Ash Sueh Hua,<sup>a</sup> John B. Plumley,<sup>b,c</sup> Austin D. Ready,<sup>a</sup> Arnold L. Rheingold,<sup>d</sup> Thomas L. Peng,<sup>b</sup> Peter I. Djurovich,<sup>e</sup> Christopher Kerestes,<sup>b</sup> Neil A. Snyder,<sup>f</sup> Andrew Andrews,<sup>f</sup> Justin R. Caram,<sup>a\*</sup> and Alexander M. Spokoyny<sup>a\*</sup>

---

<sup>a</sup> Department of Chemistry and Biochemistry and California NanoSystems Institute (CNSI), University of California, Los Angeles, California 90095, USA

<sup>b</sup> Space Vehicles Directorate, Air Force Research Laboratory, Kirtland AFB, New Mexico 87117, USA

<sup>c</sup> Center for Micro-Engineered Materials, University of New Mexico, Albuquerque, New Mexico 87106, USA

<sup>d</sup> Department of Chemistry, University of California, San Diego, 9500 Gilman Drive, La Jolla, California 92093, USA

<sup>e</sup> USA Department of Chemistry, University of Southern California, Los Angeles, California 90089, USA

<sup>f</sup> BlueHalo, Albuquerque, New Mexico 87110, USA

\*E-mail: [spokoyny@chem.ucla.edu](mailto:spokoyny@chem.ucla.edu); [jcaram@chem.ucla.edu](mailto:jcaram@chem.ucla.edu)

Supporting Information (SI)

## Contents

General Considerations.....	2
Instrumentation .....	2
Experimental.....	3
Structural Characterization.....	4
NMR and MS .....	4
Crystal Structure Data .....	7
Polymer screen .....	8
Photoluminescent Characterization of Samples.....	9
Investigation of Luminescence in Different Solvents.....	11
Photoluminescence Data .....	11
NMR Data.....	12
Photostability studies.....	18
Inductively-Coupled Plasma – Optical Emission Spectroscopy (ICP-OES) Studies.....	29
UV Imaging Test .....	31
Calculations.....	31
References .....	39

## General Considerations

Aluminum chloride (Sigma-Aldrich), bromine (Oakwood), iodine (Spectrum), trifluoroacetic acid (Fisher Chemical), hydrochloric acid (Fisher Chemical), toluene (Sigma-Aldrich), benzophenone (Oakwood), poly(methyl methacrylate, 35 kDa) (Acros Organics), poly(lauryl methacrylate) 25 wt% in toluene (Sigma-Aldrich), ethyl vinyl acetate copolymer: 18 wt% vinyl acetate (Sigma-Aldrich), and polystyrene (Aldrich, Catalog No. 43011-0) were used as received. *Anti*-B<sub>18</sub>H<sub>22</sub> was isolated from a mixture of *syn*-B<sub>18</sub>H<sub>22</sub> and *anti*-B<sub>18</sub>H<sub>22</sub> isomers (Boron Specialties) by repeated recrystallizations in cyclohexane. Deuterated solvents were purchased from Cambridge Isotope Laboratories and used as received. All experiments were performed air and moisture free under an atmosphere of nitrogen using standard Schlenk techniques unless otherwise stated. Anhydrous dichloromethane used for reactions was purified on a JC Meyer Glass Contour Solvent Drying System. All post-Schlenk work-up and characterization was conducted under ambient conditions.

## Instrumentation

**General:** <sup>1</sup>H NMR and <sup>11</sup>B NMR spectra were obtained on a Bruker DRX500 spectrometer or Bruker AV400; MestreNova software was used to process the NMR data. <sup>1</sup>H NMR spectra were

referenced to residual solvent resonances in deuterated solvents ( $\text{CDCl}_3$ :  $\delta$  7.26 ppm).  $^{11}\text{B}$  NMR spectra were referenced to  $\text{BF}_3 \cdot \text{Et}_2\text{O}$  ( $\delta$  0 ppm) standard. Mass spectra were obtained using a direct inject method on a Waters LCT Premier Mass Spectrometer (MS) with a Waters ACQUITY UPLC System and autosampler. UV–Vis spectra were recorded on an Ocean Optics DH-2000 spectrometer. Photoluminescence spectra were measured using a QuantaMaster Photon Technology International phosphorescence/fluorescence spectrofluorimeter. Quantum yield measurements were carried out using a Hamamatsu C9920 system equipped with a xenon lamp, calibrated integrating sphere, and model C10027 photonic multichannel analyzer (PMA). Photoluminescence lifetimes were measured by time-correlated single-photon counting using an IBH Fluorocube instrument equipped with an LED excitation source. The following equipment for the UV imaging setup was purchased from ThorLabs: Unmounted LED (LED340W) and 340 nm bandpass filter (FB340-10). For the photostability studies, the excitation source is a 266 nm laser (Teem Photonics SNU-20F-10C) with pulse repetition rate of 20 KHz, 0.6nm pulse width and a maximum average power of 20 mW. The emission is collected to a 200  $\mu\text{m}$  multimode UV fiber coupled to an imaging spectrometer (Acton 2300) equipped with an TE cooled camera (Andor Newton).

## Experimental

**Synthesis of 4,4'-Br<sub>2</sub>-anti-B<sub>18</sub>H<sub>20</sub>:** *Anti*-B<sub>18</sub>H<sub>22</sub> (100 mg, 0.46 mmol, 1.00 equiv) and AlCl<sub>3</sub> (9 mg, 0.07 mmol, 50 mol%) were charged to a dry 10 mL reaction tube equipped with a stir bar. Dry dichloromethane (8 mL) was added, and the slurry was stirred and sonicated for approx. 5 min until most of the solid was dissolved. Br<sub>2</sub> (147 mg, 0.92 mmol, 2 equiv) was added under a flow of N<sub>2</sub> and the reaction mixture was stirred at ambient temperature for 1 hr, or until the reaction was pale orange in color. The presence of B<sub>18</sub>H<sub>20</sub>Br<sub>2</sub> and B<sub>18</sub>H<sub>19</sub>Br<sub>3</sub> was detected by electrospray ionization mass spectrometry (ESI(-) MS). The reaction mixture was quenched through the addition of saturated sodium thiosulfate (5 mL) and then transferred into a separatory funnel. An aqueous solution of saturated sodium bicarbonate (2 mL) was added, and the organic phase was extracted from the biphasic solution with Et<sub>2</sub>O (5x15 mL). The organic solution was dried over MgSO<sub>4</sub> and vacuum filtered through a filter frit packed with Celite. The solvent was removed under reduced pressure to yield a yellow solid. Pure B<sub>18</sub>H<sub>20</sub>Br<sub>2</sub> was obtained by dissolving the solid in a minimal amount of boiling benzene, which was slowly cooled to room temperature and then to 5°C. Alternatively, column chromatography can be conducted on silica (activated with a solution of 5% TFA in hexanes) using hexanes as a mobile phase, R<sub>f</sub> = 0.40. Crystals of suitable quality for a single crystal X-ray diffraction study were grown by dissolution of pure product in hot benzene followed by cooling the solution to room temperature and its storage at ~5 °C for 5 days. 4,4'-Br<sub>2</sub>-anti-B<sub>18</sub>H<sub>20</sub> was isolated in 74% yield (101 mg).  $^1\text{H}\{^{11}\text{B}\}$  NMR (500 MHz,  $\text{CDCl}_3$ ):  $\delta$  4.48 (2H, s), 4.25 (2H, s), 3.88 (2H, s), 3.48 (2H, s), 3.39 (2H, s), 3.07 (2H, s), 0.16 (2H, s), 0.07 (2H, s), -0.90 (2H, s), -2.06 (2H, s) ppm.  $^{11}\text{B}\{^1\text{H}\}$  NMR (160 MHz,  $\text{CDCl}_3$ ):  $\delta$  16.12 (2B, s), 9.73 (2B, s), 3.26 (4B, s), 1.70 (2B, s), -2.70 (2B, s), -11.63 (2B, s), -30.85 (2B, s), -31.25 (2B, s) ppm. **ESI(-) MS**  $m/z$ : 374.1596 (calc. 374.1622).

**Synthesis of 4,4-I<sub>2</sub>-anti-B<sub>18</sub>H<sub>20</sub>:** This compound was synthesized according to a previously reported procedure.<sup>1</sup>

# Structural Characterization

## NMR and MS

### $^1\text{H}\{^{11}\text{B}\}$ NMR

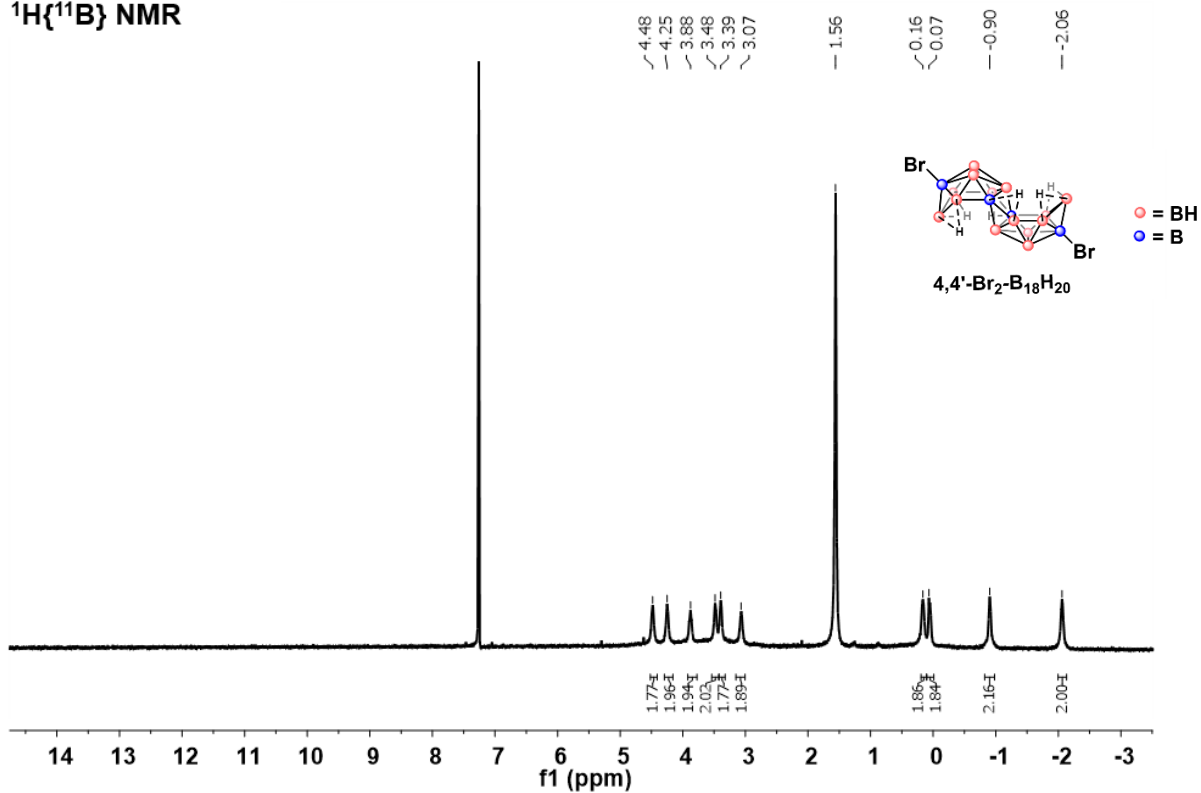


**Figure S1.**  $^1\text{H}\{^{11}\text{B}\}$  NMR spectrum in  $\text{CDCl}_3$  of  $4,4'\text{-Br}_2\text{-anti-B}_{18}\text{H}_{20}$  in  $\text{CDCl}_3$ .

$^{11}\text{B}\{^1\text{H}\}$  NMR

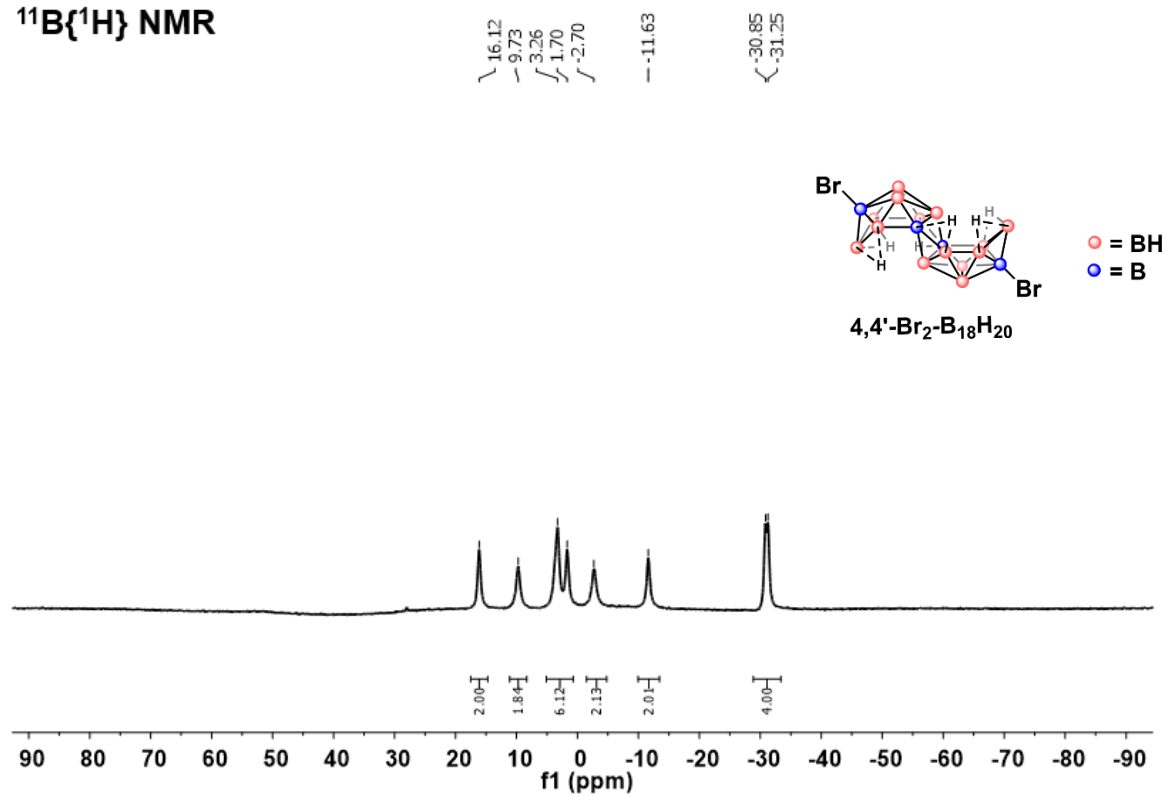


**Figure S2.**  $^{11}\text{B}\{^1\text{H}\}$  NMR spectrum in  $\text{CDCl}_3$  of  $4,4'\text{-Br}_2\text{-anti-B}_{18}\text{H}_{20}$  in  $\text{CDCl}_3$ .

# $^{11}\text{B}$ NMR

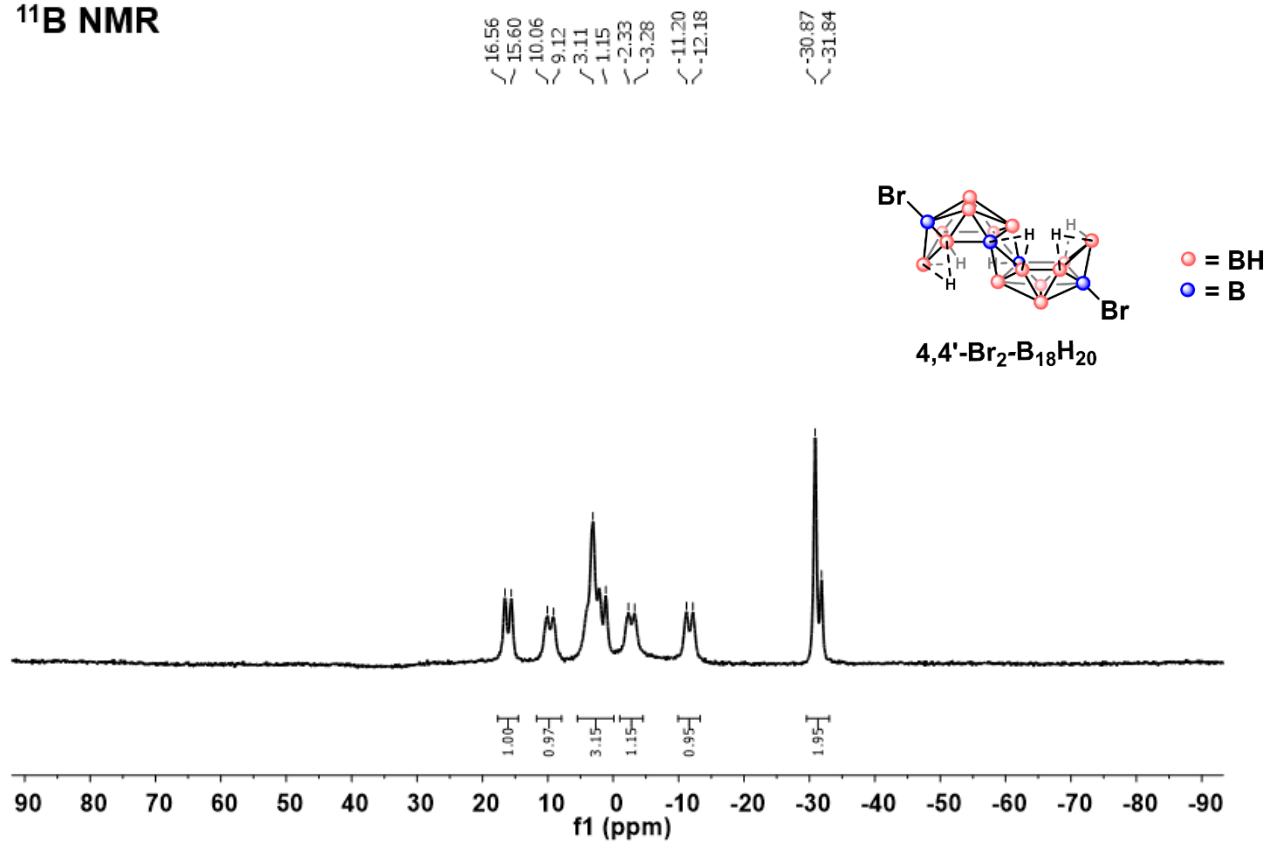


**Figure S3.**  $^{11}\text{B}$  NMR spectrum in  $\text{CDCl}_3$  of  $4,4'\text{-Br}_2\text{-anti-B}_{18}\text{H}_{20}$  in  $\text{CDCl}_3$ .

## ESI(-) MS

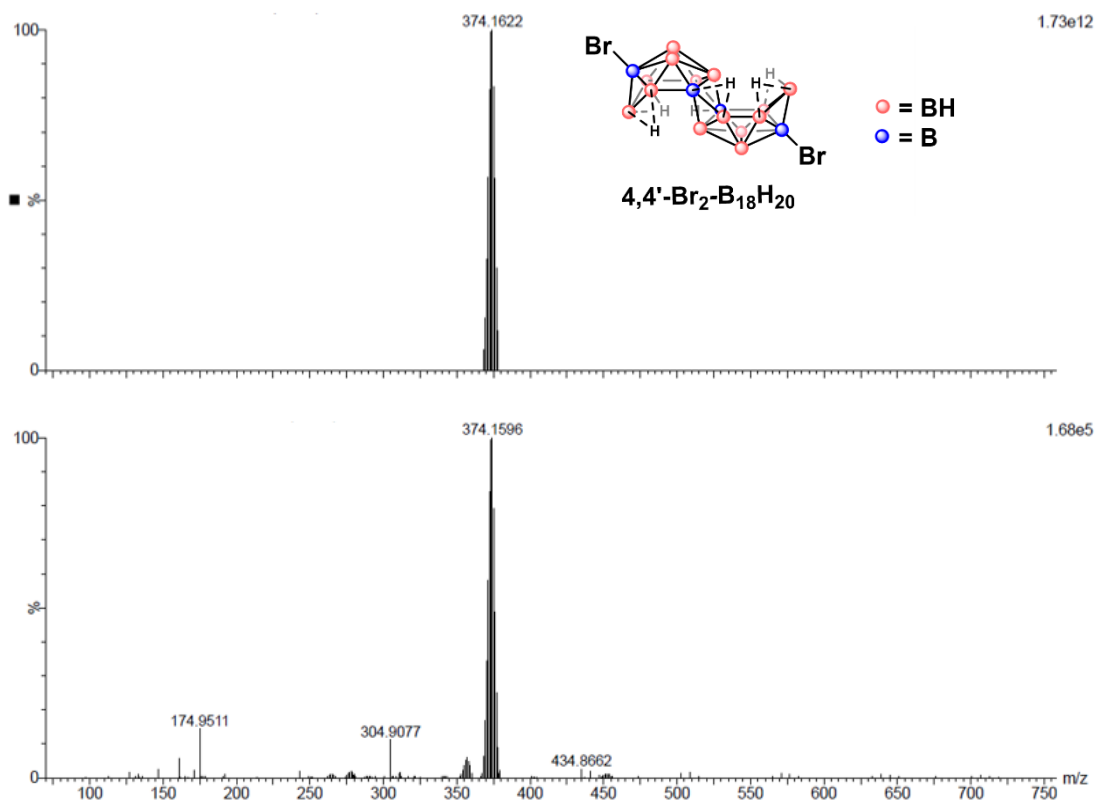


**Figure S4.** Predicted (top) and experimental (bottom) ESI(-) MS of 4,4'-Br<sub>2</sub>-anti-B<sub>18</sub>H<sub>20</sub>

## Crystal Structure Data

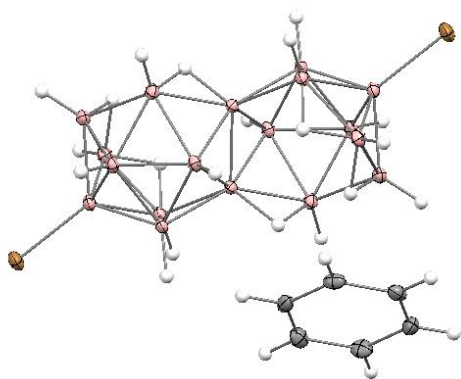


**Figure S5.** 4,4'-Br<sub>2</sub>-anti-B<sub>18</sub>H<sub>20</sub> single crystal X-ray structure with a co-crystallized benzene solvent molecule.

**Table S1.** Crystal data and structure refinement parameters for 4,4'-Br<sub>2</sub>-anti-B<sub>18</sub>H<sub>20</sub>•(C<sub>6</sub>H<sub>6</sub>), CSD# 2135549.

Identification code	KA-II-030	
Empirical formula	C <sub>6</sub> H <sub>26</sub> B <sub>18</sub> Br <sub>2</sub>	
Formula weight	452.67	
Temperature	100.0 K	
Wavelength	0.71073 Å	
Crystal system	Monoclinic	
Space group	C 2/c	
Unit cell dimensions	$a = 18.6214(7)$ Å	$\alpha = 90^\circ$ .
	$b = 10.4194(3)$ Å	$\beta = 99.341(2)^\circ$ .
	$c = 10.7159(4)$ Å	$\gamma = 90^\circ$ .
Volume	2051.57(12) Å <sup>3</sup>	
Z	4	
Density (calculated)	1.466 Mg/m <sup>3</sup>	
Absorption coefficient	3.939 mm <sup>-1</sup>	
F(000)	888	
Crystal size	0.26 x 0.25 x 0.23 mm <sup>3</sup>	
Theta range for data collection	2.217 to 27.148°.	
Index ranges	-18<= <i>h</i> <=23, -13<= <i>k</i> <=12, -13<= <i>l</i> <=12	
Reflections collected	7251	
Independent reflections	2266 [ <i>R</i> (int) = 0.0397]	
Completeness to theta = 25.242°	99.8 %	
Absorption correction	Semi-empirical from equivalents	
Max. and min. transmission	0.3330 and 0.2770	
Refinement method	Full-matrix least-squares on <i>F</i> <sup>2</sup>	
Data / restraints / parameters	2266 / 0 / 147	
Goodness-of-fit on <i>F</i> <sup>2</sup>	1.101	
Final <i>R</i> indices [ <i>I</i> >2σ( <i>I</i> )]	<i>R</i> 1 = 0.0227, <i>wR</i> 2 = 0.0595	
<i>R</i> indices (all data)	<i>R</i> 1 = 0.0256, <i>wR</i> 2 = 0.0607	
Extinction coefficient	n/a	
Largest diff. peak and hole	0.579 and -0.241 e.Å <sup>-3</sup>	

## Polymer screen

**Preparation of thin films on quartz:** 50 mg polymer (either PMMA, PLMA, EVA, or PS) was dissolved in 2 mL toluene (dichloromethane for EVA solubility) under ambient conditions. Solutions were sonicated at 40°C until polymer was fully dissolved. Emitter (1 mg) was added to give a 2 wt% solution. The solution was dropcast in an even layer onto a clean 1x1 inch quartz substrate using a glass pipet and dried over 24 hrs.

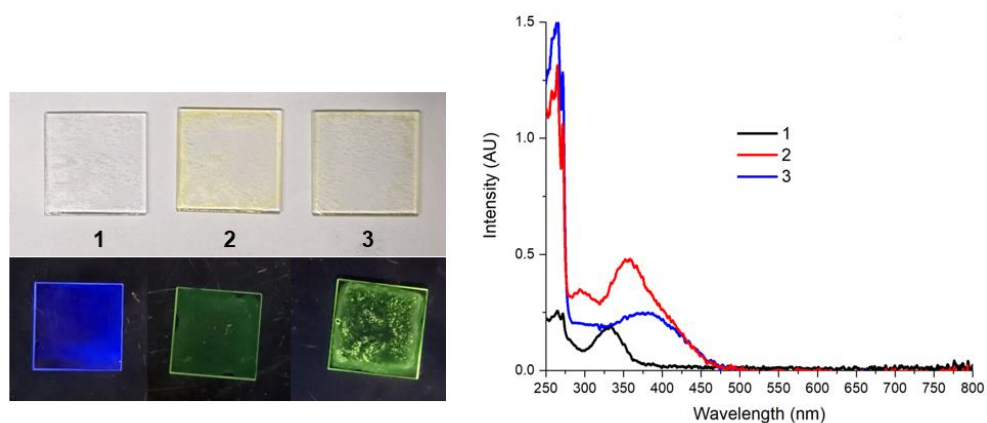


**Figure S6.** Left: 2 wt% PMMA films of **1-3** under ambient lighting and UV light. Right: Absorbance spectra of PMMA films **1-3**.

### Photoluminescent Characterization of Samples

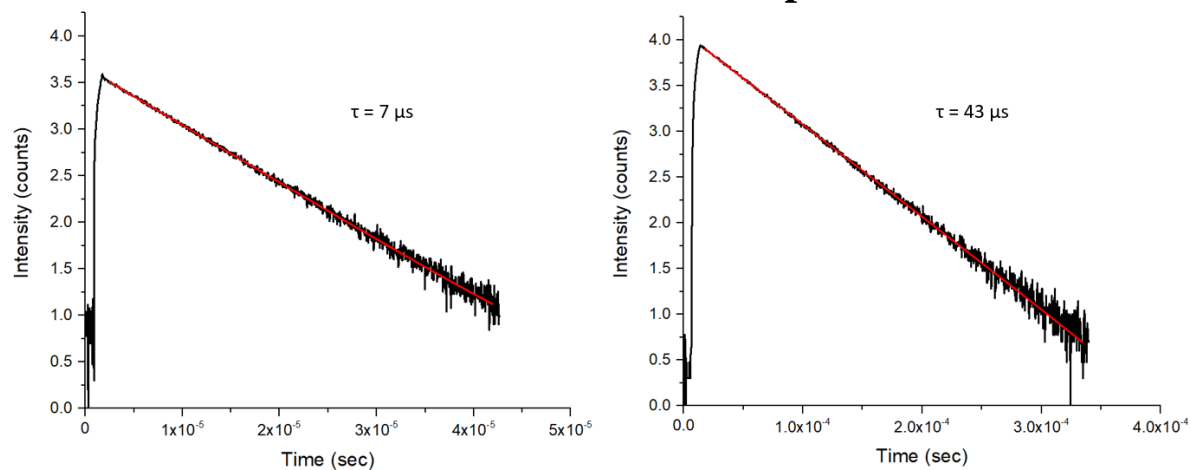


**Figure S7.** Lifetime of **2** in cyclohexane solution (left) and oxygen-free cyclohexane (right).

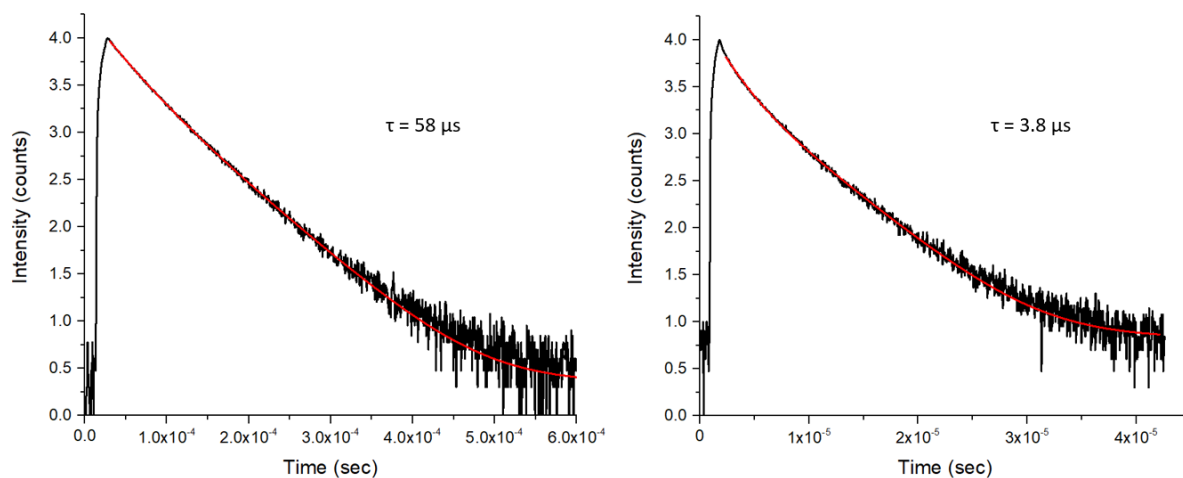


**Figure S8.** Lifetime of toluene-prepared polystyrene films of **2** (left) and **3** (right) under vacuum (due to an error the lifetime of toluene-prepared polystyrene films of **1** was incorrect).

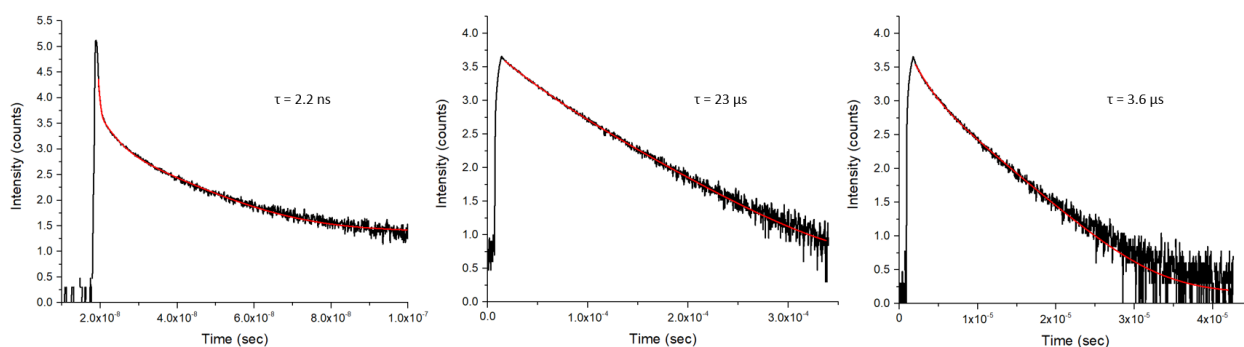


**Figure S9.** Lifetime of dichloromethane prepared polystyrene films, left to right, of **1**, **2**, and **3** under vacuum.

**Table S2.** Photophysical data from the dichloromethane-prepared polystyrene films. Emission ( $\lambda_{em}$ ), quantum yield ( $\Phi$ ), lifetime ( $\tau$ ), and radiative ( $k_r = \Phi_{film}^a / \tau_{film}$ ) and non-radiative ( $k_{nr} = (1 - \Phi_{film}^a) / \tau_{film}$ ) decay rates for **1-3**. <sup>a</sup>Under nitrogen atmosphere, <sup>b</sup>Under vacuum. Excitation wavelength ( $\lambda_{exc}$ ) = 340 nm for emission and quantum yield,  $\lambda_{exc}$  = 331 nm for **1** and 405 nm for **2** and **3**.

	<i>Anti-B<sub>18</sub>H<sub>22</sub></i>	<i>4,4'-Br<sub>2</sub>-anti-B<sub>18</sub>H<sub>20</sub></i>	<i>4,4'-I<sub>2</sub>-anti-B<sub>18</sub>H<sub>20</sub></i>
$\Phi_{film}$	0.18	0.28	0.30
	0.19 <sup>a</sup>	0.47 <sup>a</sup>	0.34 <sup>a</sup>
$\tau_{film}$ ( $\mu$ s)	0.0022 <sup>b</sup>	45 <sup>b</sup>	3.6 <sup>b</sup>
$k_r$ ( $\mu$ s <sup>-1</sup> )	86	0.010	0.094
$k_{nr}$ ( $\mu$ s <sup>-1</sup> )	370	0.012	0.18

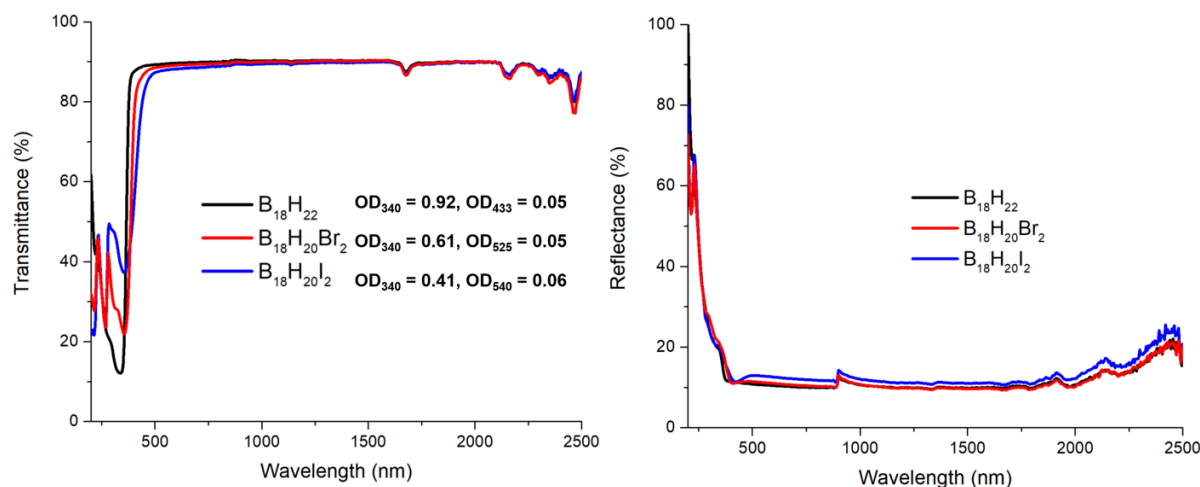


**Figure S10.** Transmittance (left) and reflectance (right) graphs of **1-3** with calculated optical densities at excitation 340 nm.

# Investigation of Luminescence in Different Solvents

## Photoluminescence Data

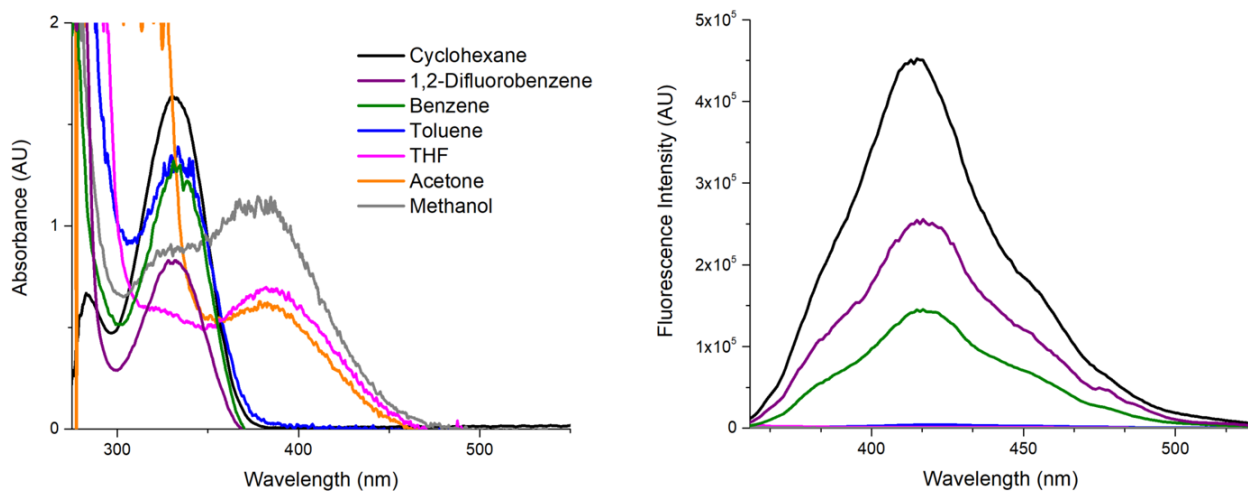


**Figure S11.** Absorbance (left) and emission (right) of **1** in various solvents. Emission spectra were obtained under ambient conditions by adding 2 mL of solvent to 0.1 mL of a  $2.3 \times 10^{-4}$  M solution of **1** in cyclohexane.  $\lambda_{\text{exc}}=340$  nm.

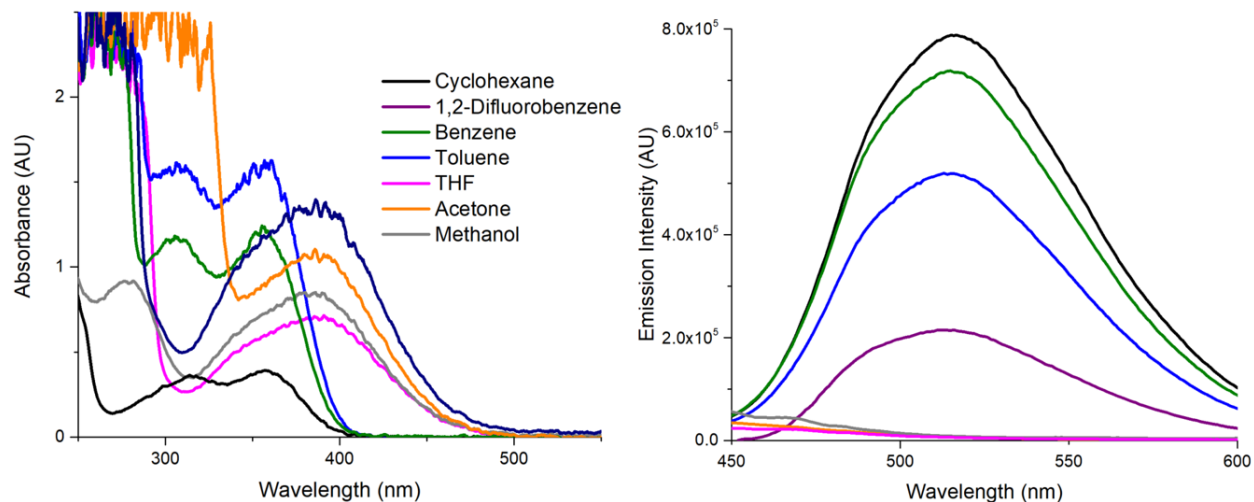


**Figure S12.** Absorbance (left) and emission (right) of **2** in various solvents. Emission spectra were obtained under ambient conditions by adding 1 mL of solvent to 0.6 mL of a  $5.4 \times 10^{-5}$  M solution of **2** in cyclohexane.  $\lambda_{\text{exc}}=340$  nm. Upward inflection of scans near 450 nm indicate the ends of Raman peaks.

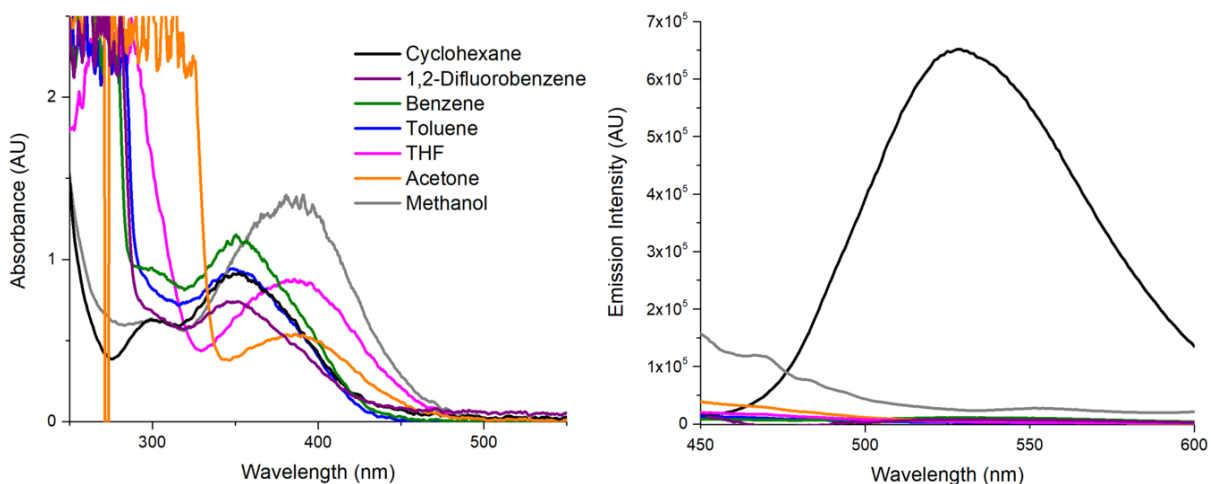


**Figure S13.** Absorbance (left) and emission (right) of **3** in various solvents. Emission spectra were obtained under ambient conditions by adding 1 mL of solvent to 0.4 mL of a  $2.6 \times 10^{-5}$  M solution of **3** in cyclohexane.  $\lambda_{\text{exc}}=340$  nm. Upward inflection of scans near 450 nm indicate the ends of Raman peaks.

## NMR Data

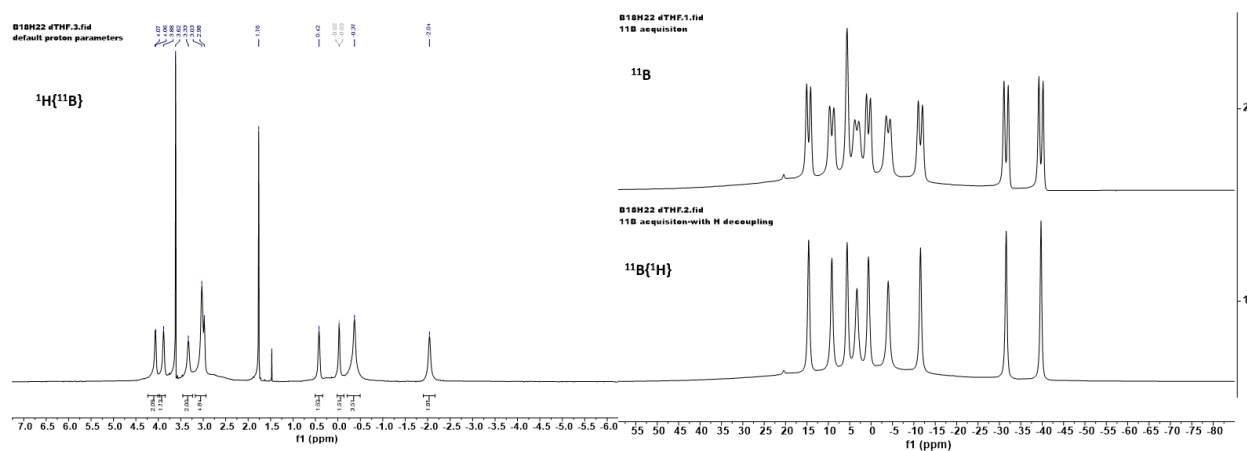


**Figure S14.** NMR spectra of **1** in tetrahydrofuran-*d*<sub>8</sub>. Chemical shifts for <sup>11</sup>B{<sup>1</sup>H} NMR spectrum are  $\delta$  14.60, 9.19, 5.62, 3.32, 0.62, -4.00, -11.54, -31.57, -39.72 ppm.

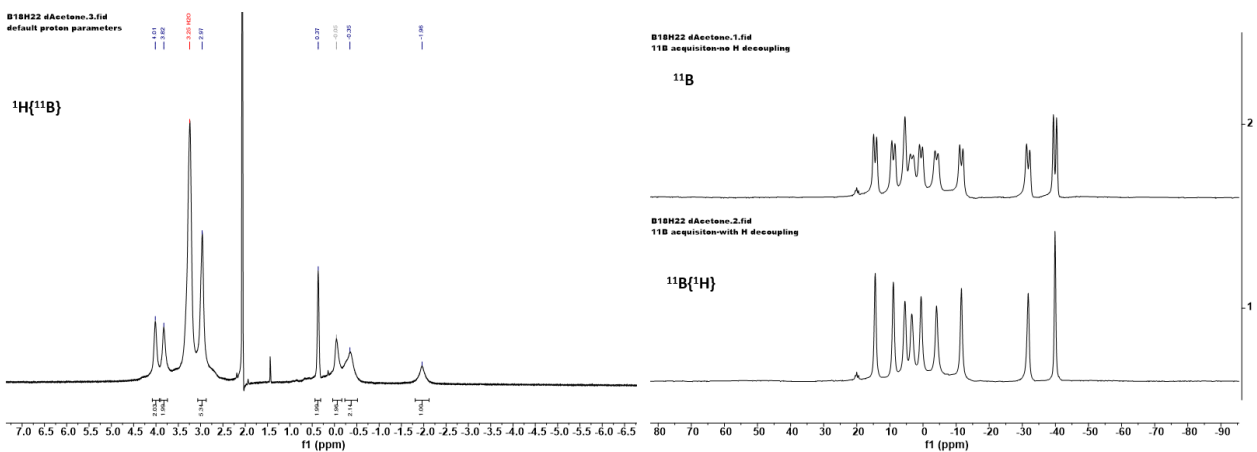


**Figure S15.** NMR spectra of **1** in acetone-*d*<sub>6</sub>. Chemical shifts for <sup>11</sup>B{<sup>1</sup>H} NMR spectrum are  $\delta$  20.03, 19.48, 14.47, 8.97, 5.49, 3.38, 0.59, -1.39, -4.09, -6.34, -11.58, -31.76, -39.90.

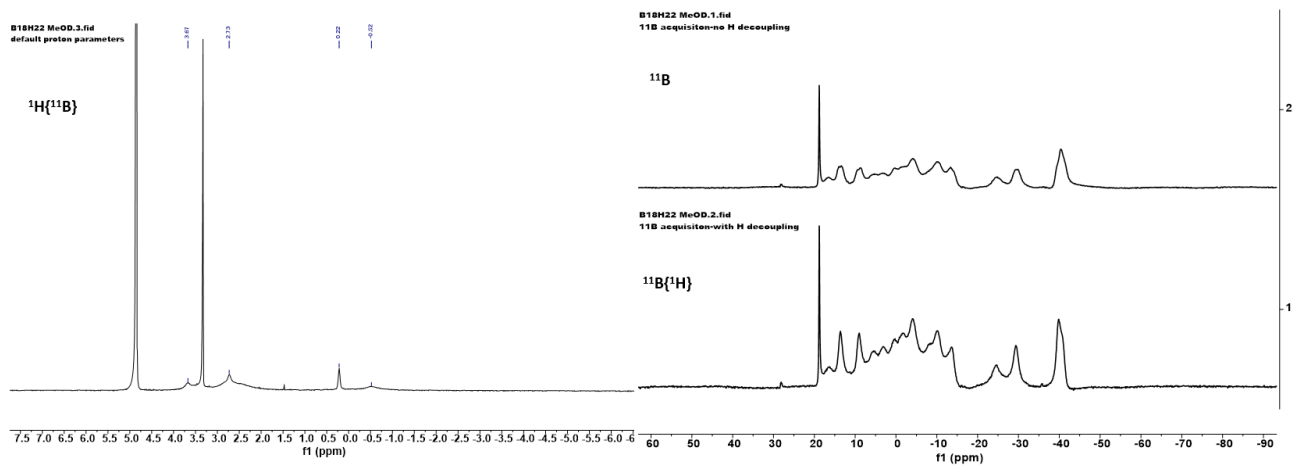


**Figure S16.** NMR spectra of **1** in methanol-*d*<sub>4</sub>. Chemical shifts for <sup>11</sup>B{<sup>1</sup>H} NMR spectrum are  $\delta$  28.18, 18.77, 16.53, 13.59, 9.02, 5.70, 3.23, 0.31, -1.70, -4.15, -10.01, -13.64, -24.52, -29.37, -39.87.

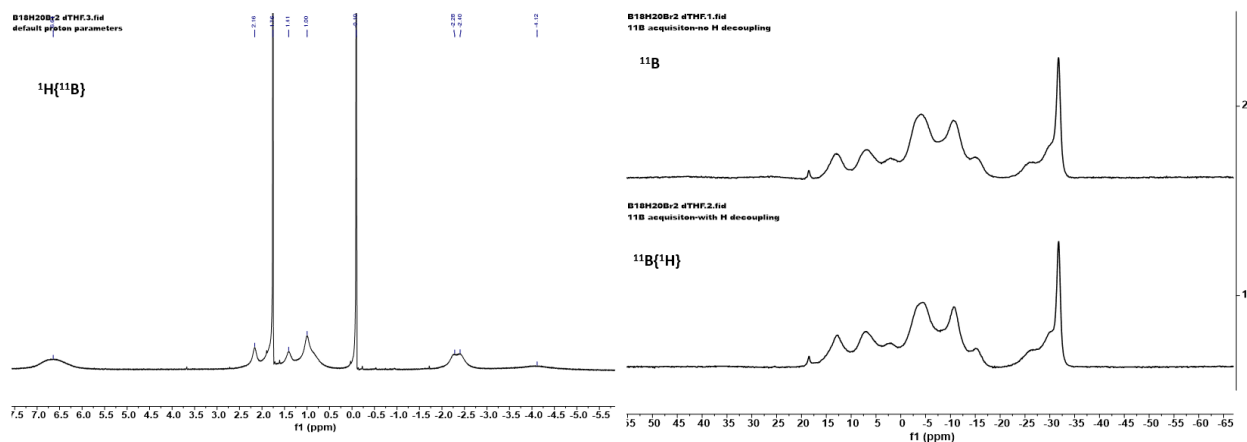


**Figure S17.** NMR spectra of **2** in tetrahydrofuran  $-d_8$ . Chemical shifts for  $^{11}\text{B}\{^1\text{H}\}$  NMR spectrum are  $\delta$  18.52, 12.87, 6.95, 2.42, -4.28, -10.72, -15.30, -31.75.

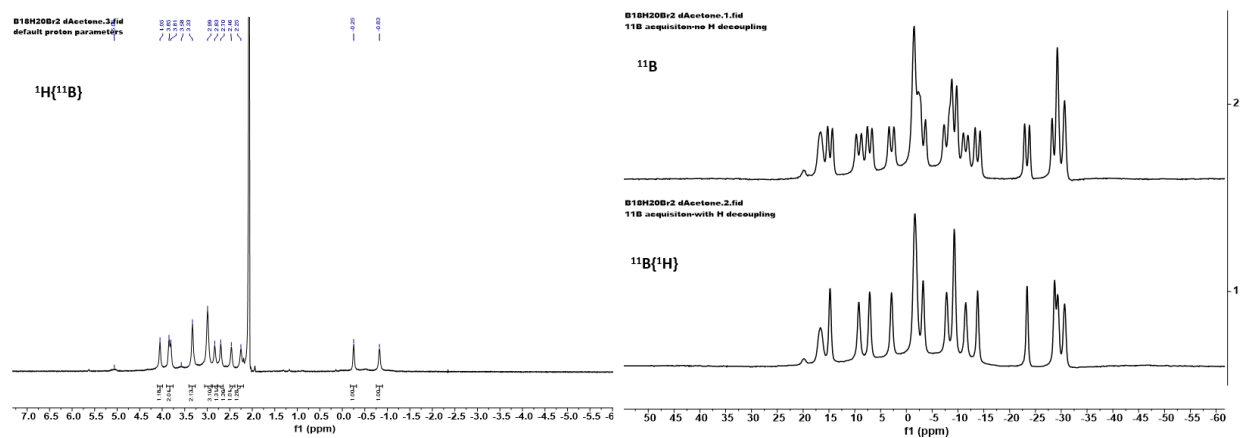


**Figure S18.** NMR spectra of **2** in acetone  $-d_6$ . Chemical shifts for  $^{11}\text{B}\{^1\text{H}\}$  NMR spectrum are  $\delta$  19.85, 16.66, 14.79, 11.56, 9.21, 7.12, 2.88, 0.98, -1.66, -3.24, -5.76, -7.79, -9.28, -11.50, -13.80, -23.38, -28.71, -29.35, -30.66.

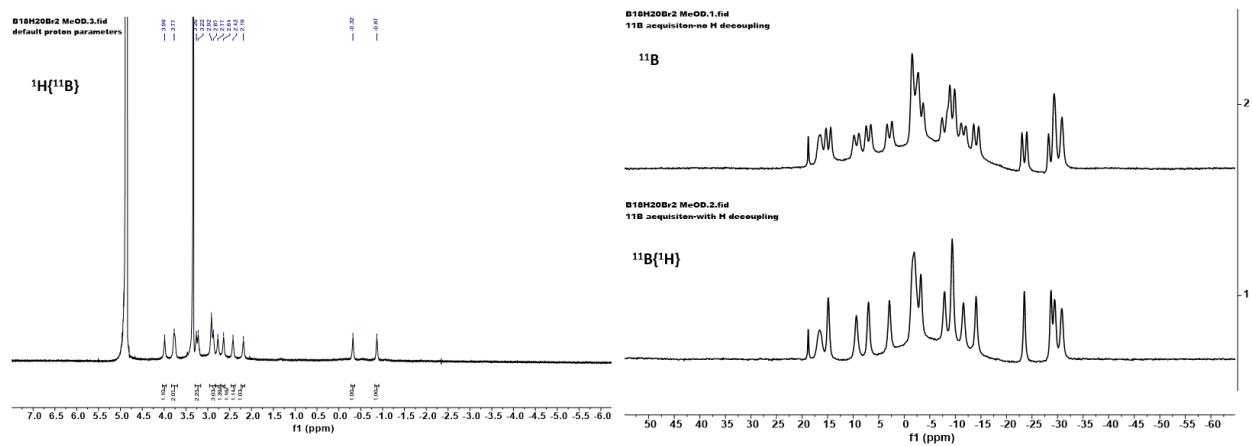


**Figure S19.** NMR spectra of **2** in methanol-*d*<sub>4</sub>. Chemical shifts for  $^{11}\text{B}\{^1\text{H}\}$  NMR spectrum are  $\delta$  18.80, 16.57, 14.87, 9.37, 7.02, 2.92, -1.36, -1.87, -3.24, -7.86, -9.39, -11.57, -14.04, -23.49, -28.70, -29.43, -30.81.

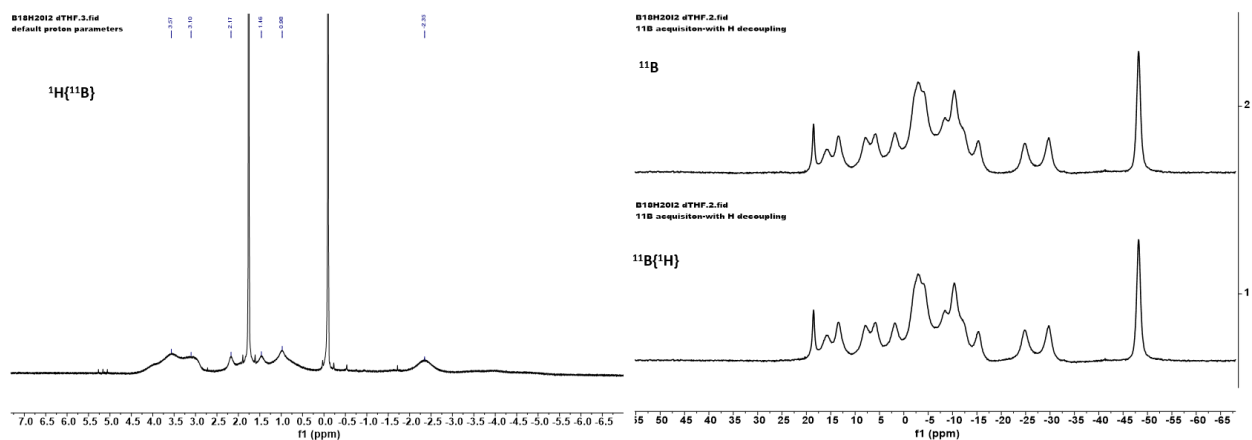


**Figure S20.** NMR spectra of **3** in tetrahydrofuran-*d*<sub>8</sub>. Chemical shifts for  $^{11}\text{B}\{^1\text{H}\}$  NMR spectrum are  $\delta$  18.54, 15.85, 13.36, 7.87, 5.86, 1.89, -3.10, -8.23, -10.43, -15.28, -24.84, -29.70, -48.17.

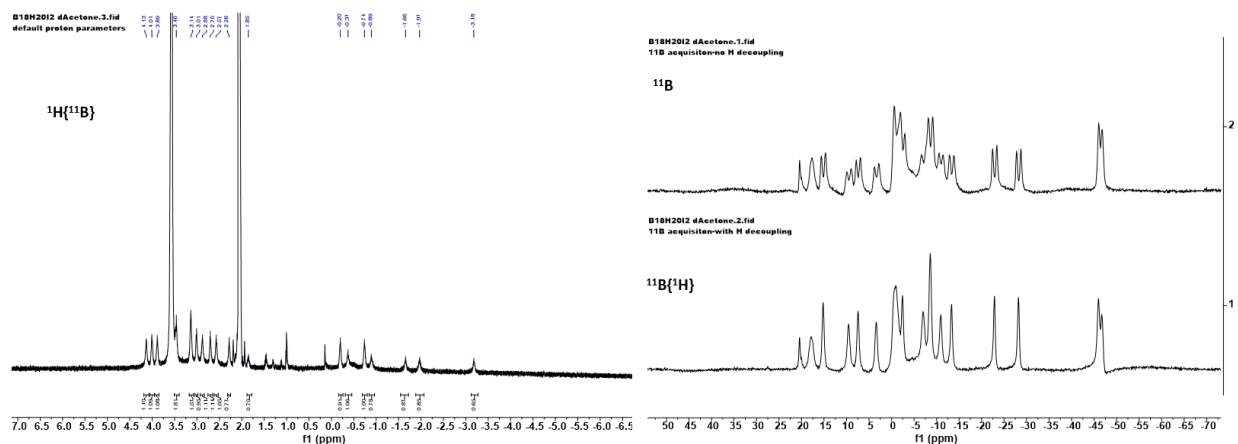


**Figure S21.** NMR spectra of **3** in acetone-*d*<sub>6</sub>. Chemical shifts for  $^{11}\text{B}\{^1\text{H}\}$  NMR spectrum are  $\delta$  20.46, 20.05, 17.83, 15.21, 9.55, 7.46, 3.41, -0.42, -1.00, -2.43, -7.00, -8.59, -10.91, -13.31, -22.84, -28.18, -45.93, -46.72.

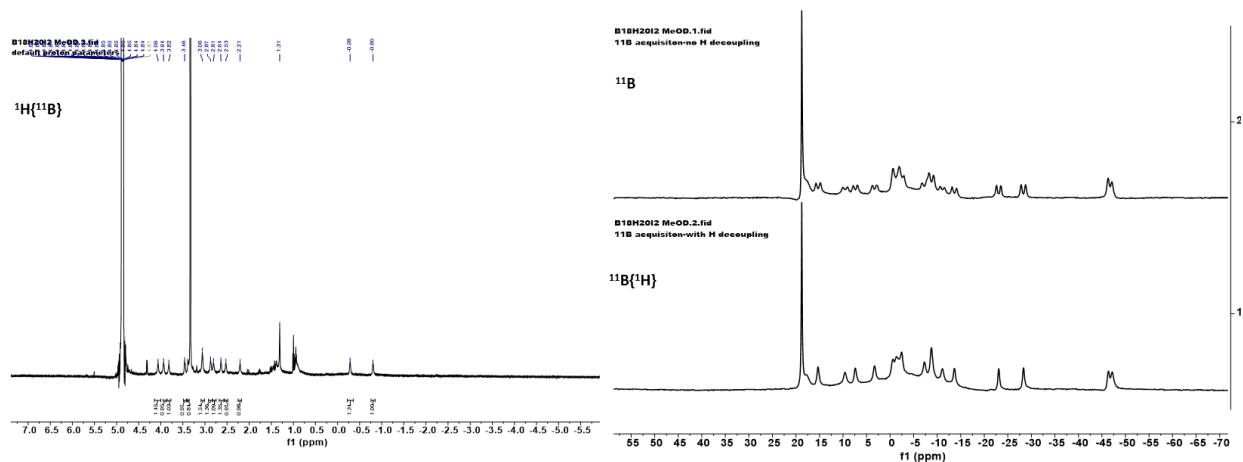


**Figure S22.** NMR spectra of **3** in methanol-*d*<sub>4</sub>. Chemical shifts for  $^{11}\text{B}\{^1\text{H}\}$  NMR spectrum are  $\delta$  18.77, 15.31, 9.60, 7.40, 3.32, -0.53, -1.39, -2.46, -7.28, -8.77, -11.09, -13.65, -23.06, -28.32, -46.34, -47.19.

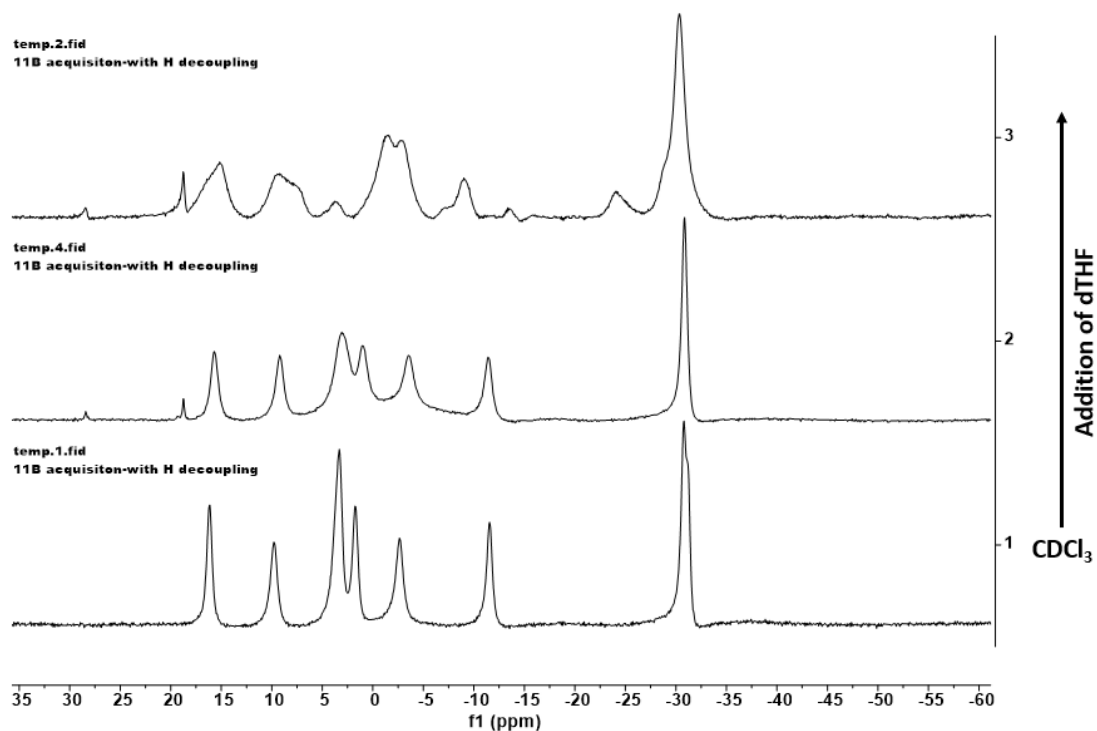


**Figure S23.**  $^{11}\text{B}\{^1\text{H}\}$  NMR spectra of **3** in  $\text{CDCl}_3$  (bottom) with successively increasing amounts of tetrahydrofuran  $-d_8$  (middle and top).

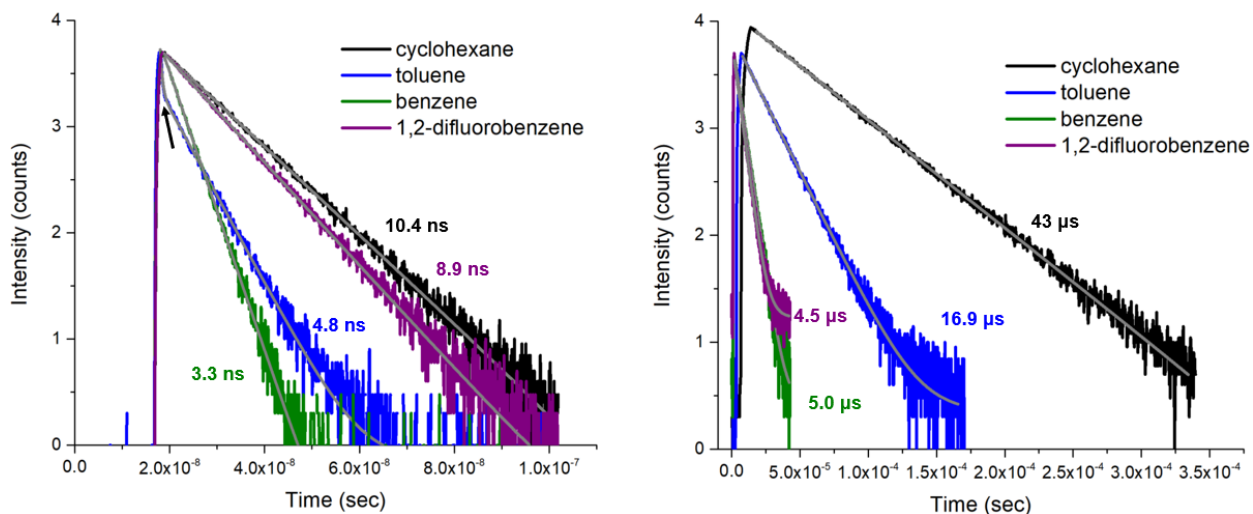


**Figure S24.** Lifetimes of **1** (left) and **2** (right) in cyclohexane, toluene, benzene, and 1,2-difluorobenzene. The arrow in the left panel indicates the non-monoexponential decay kinetics in toluene. Lifetimes of **2** were taken in degassed solutions to eliminate oxygen quenching processes.

## **Photostability studies**

**Preparation of thin films on quartz:** PMMA: 100 mg PMMA was dissolved in 2 mL toluene under ambient conditions. Emitter (2 mg) was added to give a 2 wt% solution. The solution was spin coated in an even layer onto a clean 1x1 inch quartz substrate using a glass pipet and dried over 24 hrs.

PS: 50 mg polystyrene was dissolved in 1 mL toluene under ambient conditions. Emitter (1 mg) was added to give a 2 wt% solution. The solution was dropcast in an even layer onto a clean 1x1 inch quartz substrate using a glass pipet and dried over 24 hrs.

### **Sample irradiation<sup>2</sup>**

Solar ultraviolet simulation is accomplished with an Oriel 1000 Watt solar simulator, filtered to reject wavelengths longer than 400 nm, and tuned to optimum uniformity and desired intensity by varying the working distance. An integrated photodiode sensor on the simulator tracks beam intensity levels. Continuous exposure is performed until desired equivalent sun hours (ESH) are achieved.

The power incident on each sample position is critical in determining UV exposure levels. Calibration established power levels for a set simulator operating point and sample positioning prior to a UV degradation test. Once sample layout is established, a pyranometer is used to measure the total power in Watts at each sample position. During pre-test calibration, the pyranometer is mounted, centered in the sample position, and at the same working distance from the simulator. With the simulator at the set operating point, and fully warmed up, a power measurement is taken and the process is repeated for each sample position. The photodiode sensor on the solar simulator is used to maintain expected test plane intensity levels. This is accomplished by correlating the output of the photodiode sensor to the power measurement at the test plane during the calibration process.

Post-irradiation characterization

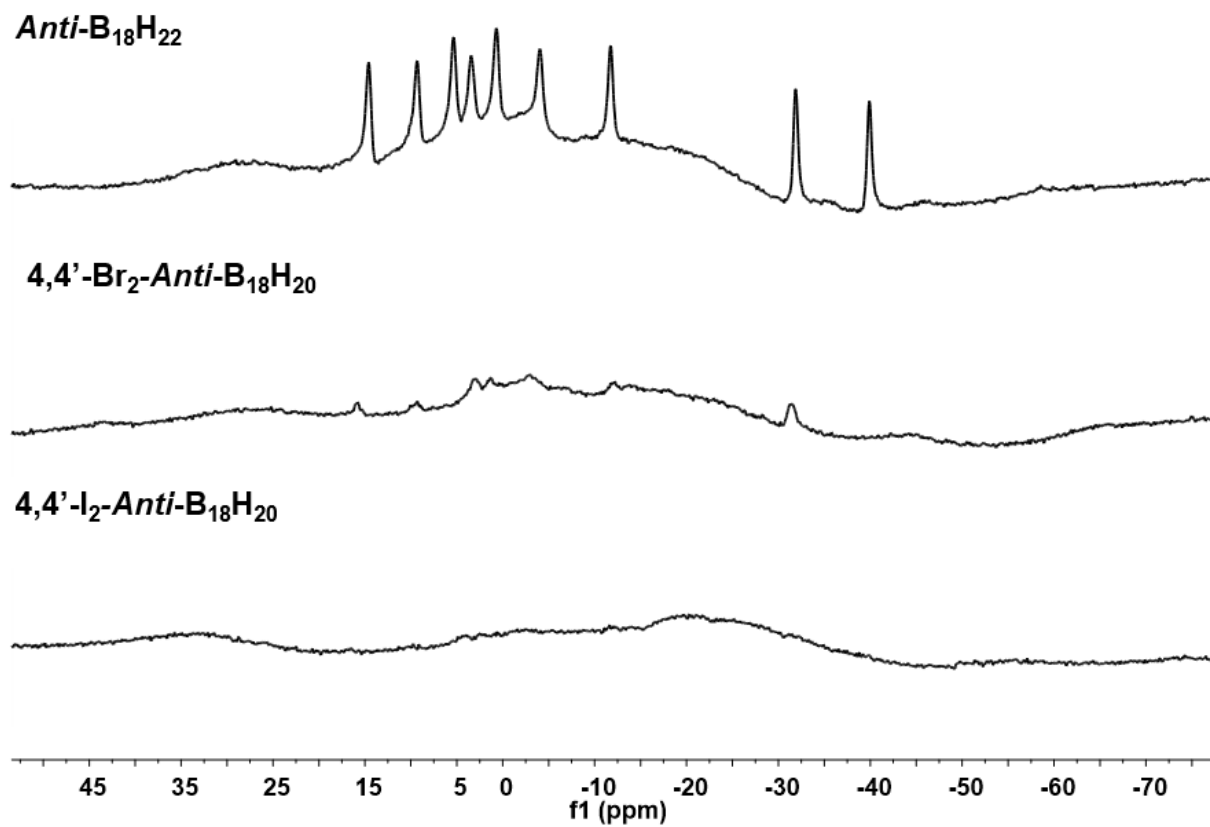


**Figure S25.**  $^{11}\text{B}\{^1\text{H}\}$  NMR spectra in  $\text{CDCl}_3$  of **PMMA-1**, **PMMA-2** and **PMMA-3** after 7 days of 266 nm light exposure.

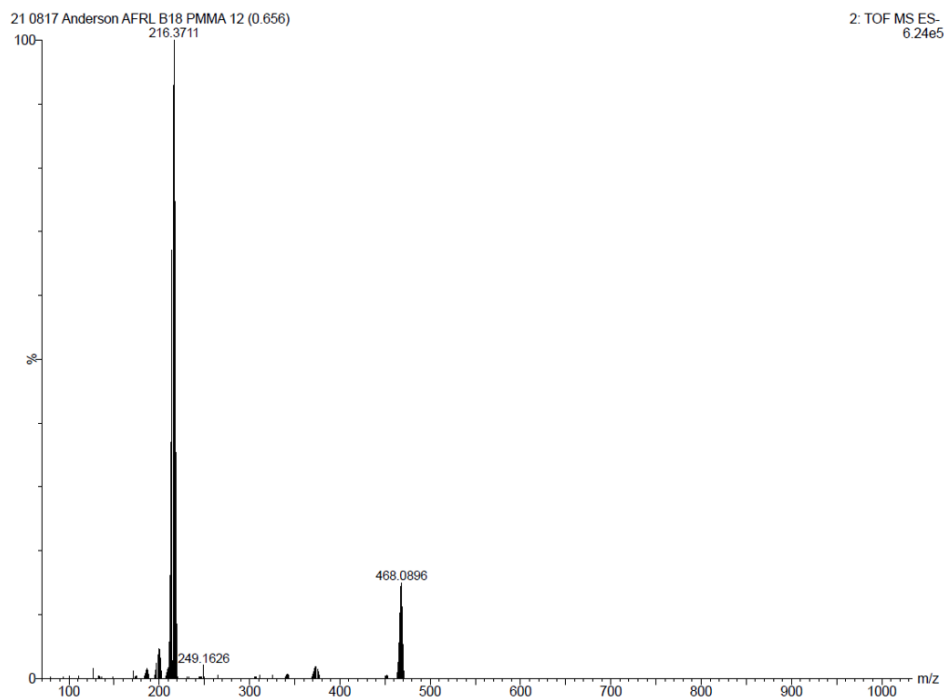


**Figure S26.** ESI(-) MS of **PMMA-1** after 7 days of 266 nm light exposure. Sample preparation in methanol.

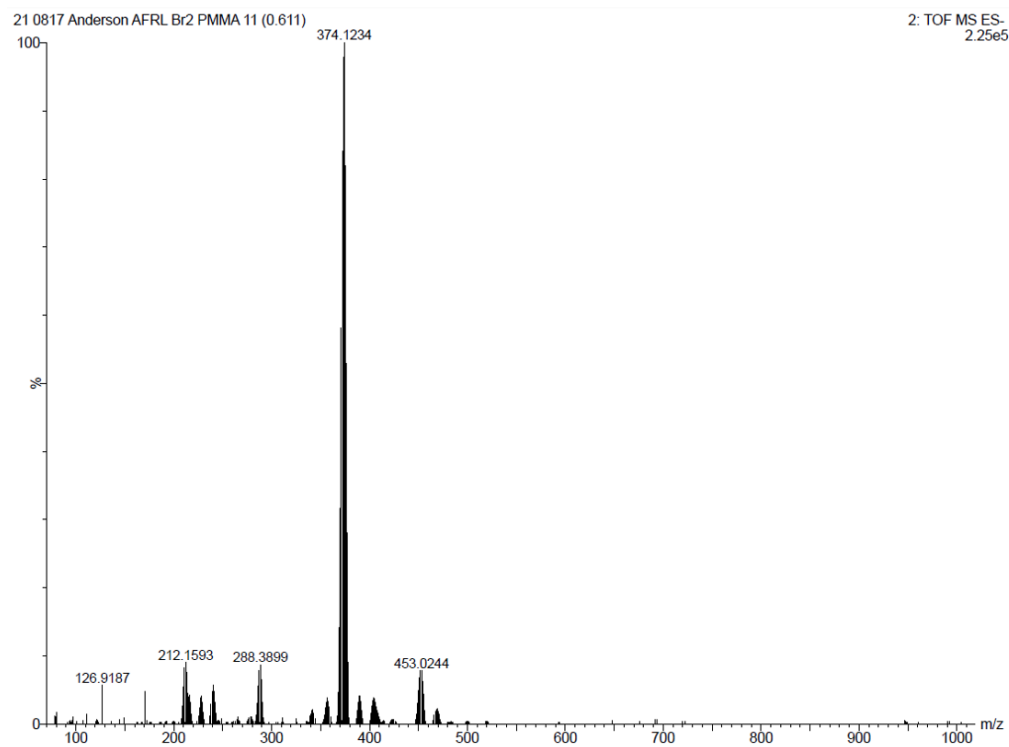


**Figure S27.** ESI(-) MS of **PMMA-2** after 7 days of 266 nm light exposure. Sample preparation in methanol.

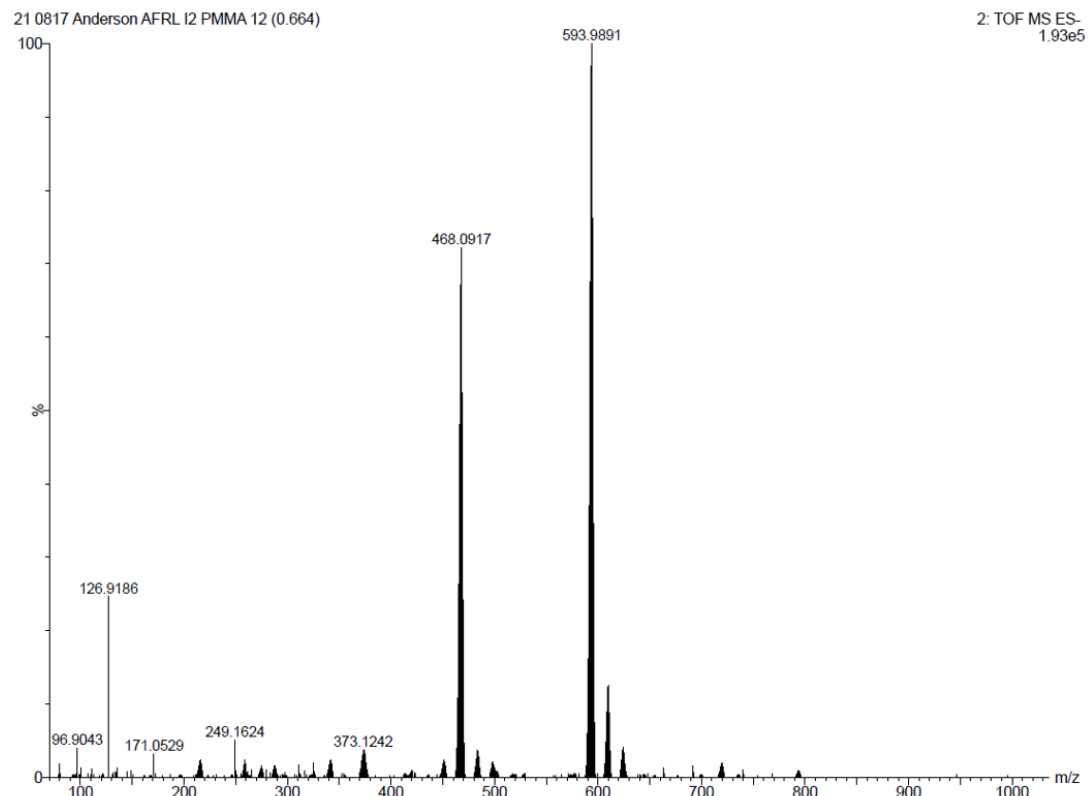


**Figure S28.** ESI(-) MS of **PMMA-3** after 7 days of 266 nm light exposure. Sample preparation in methanol.

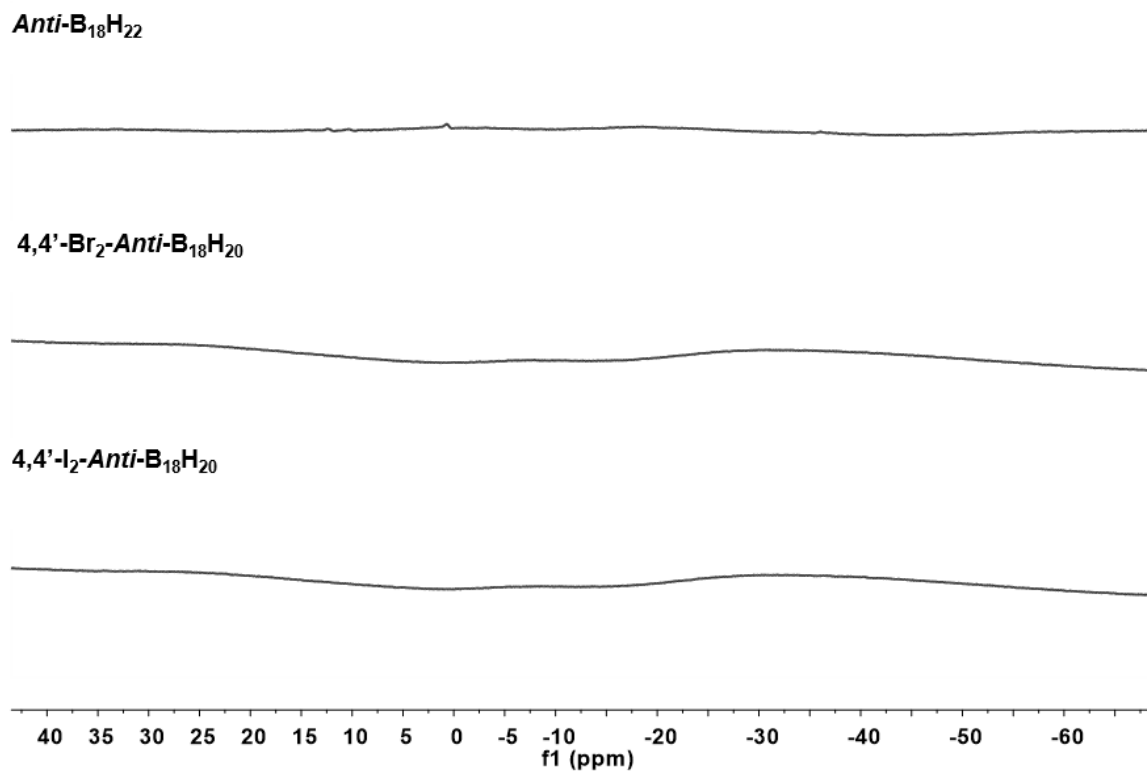


**Figure S29.**  $^{11}\text{B}\{^1\text{H}\}$  NMR spectra in  $\text{CDCl}_3$  of **PS-1**, **PS-2** and **PS-3** after 7 days of 266 nm light exposure.

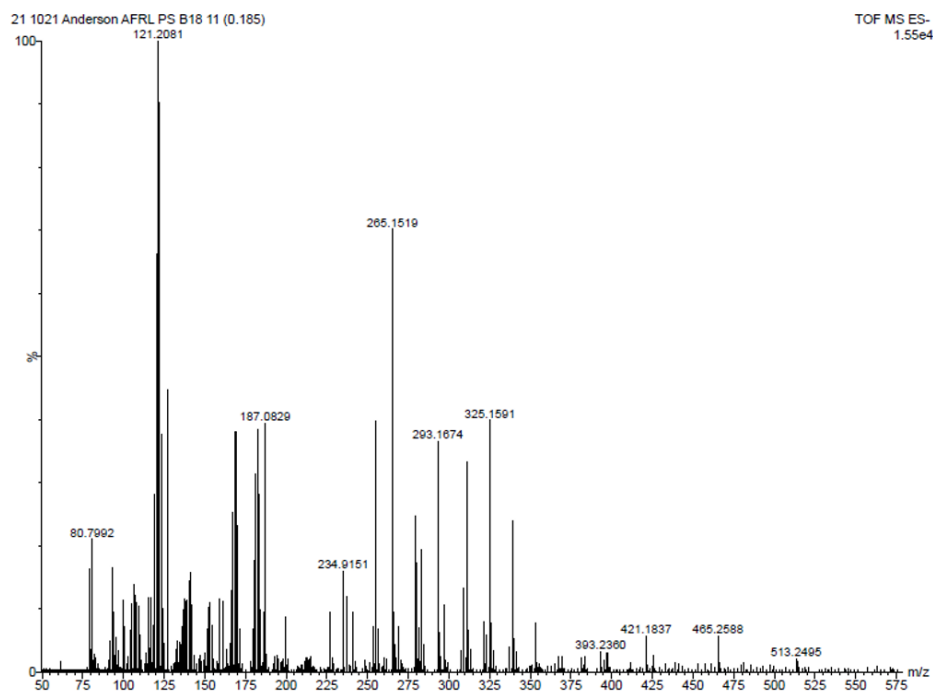


**Figure S30.** ESI(-) MS of **PS-1** after 7 days of 266 nm light exposure. Sample preparation in methanol, with insoluble polystyrene filtered off prior to sample injection.

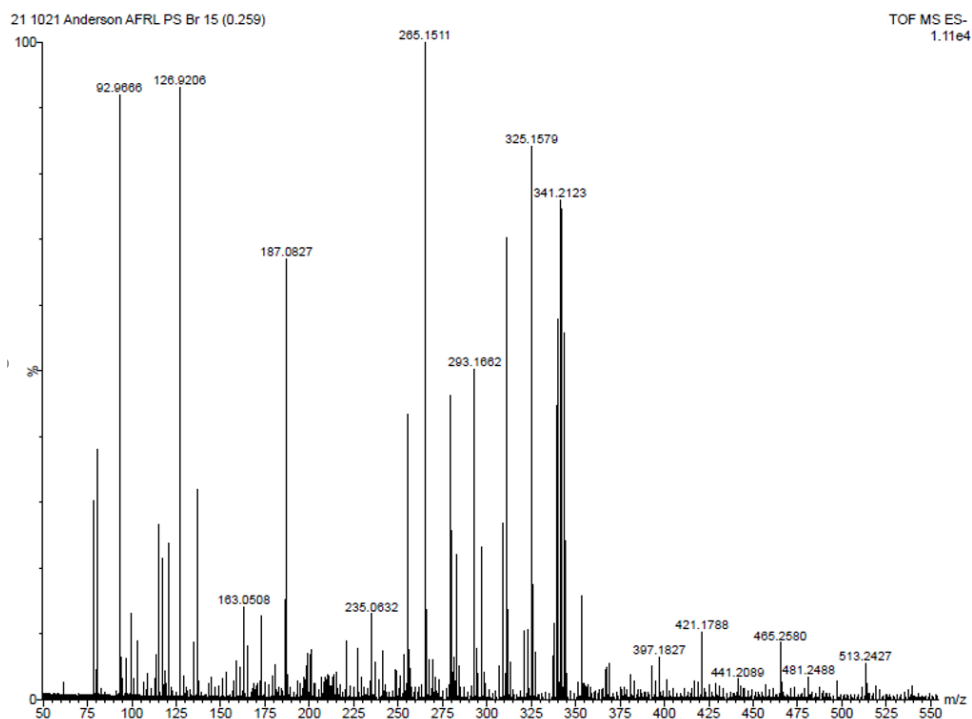


**Figure S31.** ESI(-) MS of PS-2 after 7 days of 266 nm light exposure. Sample preparation in methanol, with insoluble polystyrene filtered off prior to sample injection.

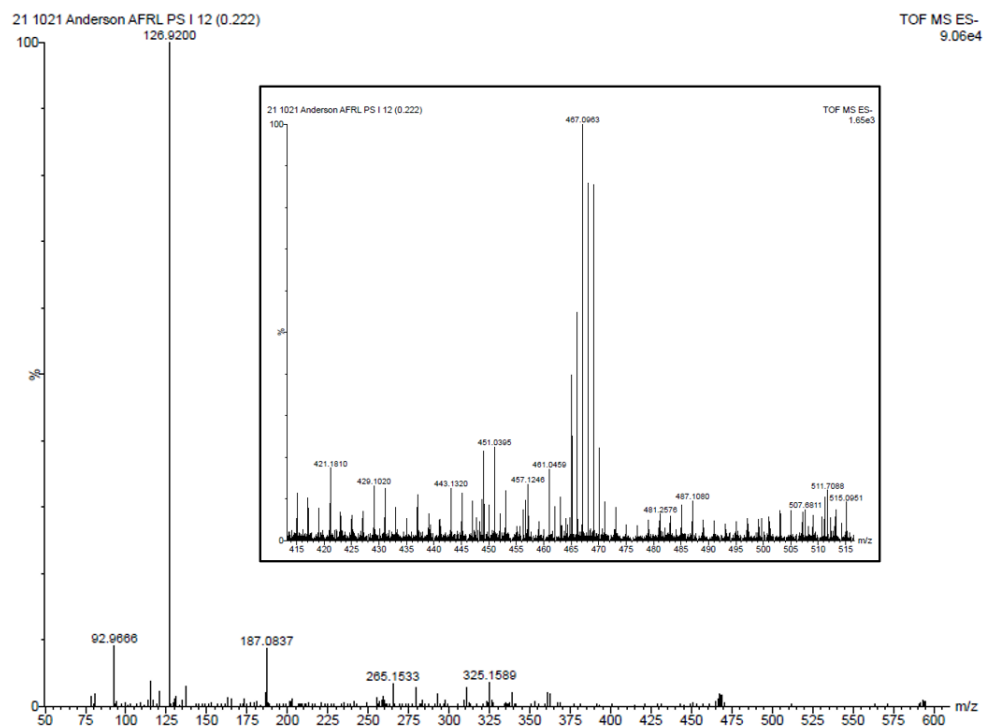


**Figure S32.** ESI(-) MS of PS-3 after 7 days of 266 nm light exposure. Sample preparation in methanol, with insoluble polystyrene filtered off prior to sample injection.

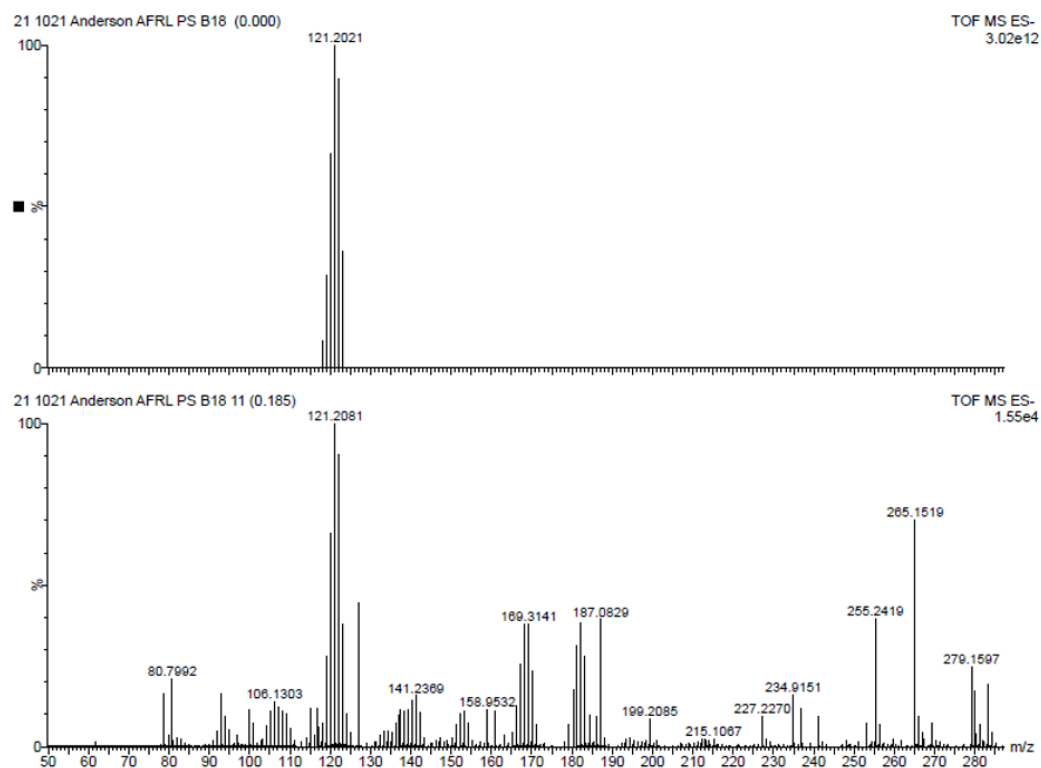


**Figure S33.** Predicted ESI(-) MS of B<sub>10</sub>H<sub>14</sub> (top) and experimental ESI(-) MS of **PS-1** (bottom) after 7 days of 266 nm light exposure. Sample preparation in methanol, with insoluble polystyrene filtered off prior to sample injection.

**Anti-B<sub>18</sub>H<sub>22</sub>**



**4,4'-Br<sub>2</sub>-Anti-B<sub>18</sub>H<sub>20</sub>**



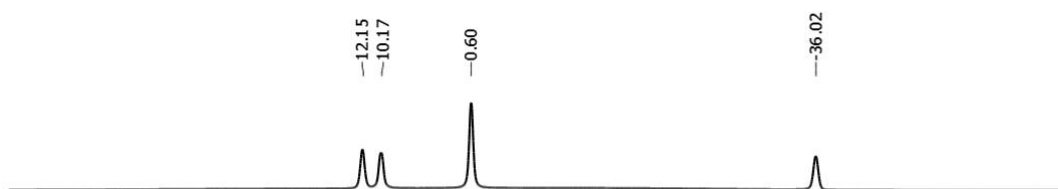
**4,4'-I<sub>2</sub>-Anti-B<sub>18</sub>H<sub>20</sub>**



45 35 25 15 5 0 -10 -20 -30 -40 -50 -60 -70  
f1 (ppm)

**Figure S34.** <sup>11</sup>B{<sup>1</sup>H} NMR spectra in CDCl<sub>3</sub> of closed vessel **PS-1**, **PS-2**, and **PS-3** after 7 days of 266 nm light exposure.

$B_{10}H_{14}$



*Anti*- $B_{18}H_{22}$  PS  
(Closed vessel)

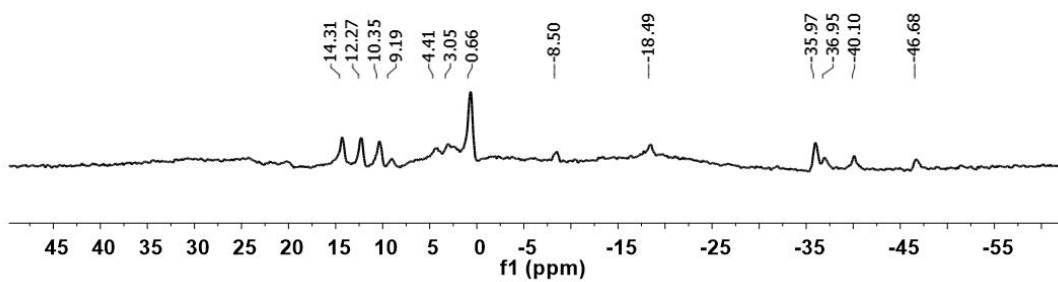


**Figure S35.**  $^{11}B\{^1H\}$  NMR spectra in  $CDCl_3$  of decaborane  $B_{10}H_{14}$  (top) and closed vessel **PS-1** (bottom) after 7 days of 266 nm light exposure.

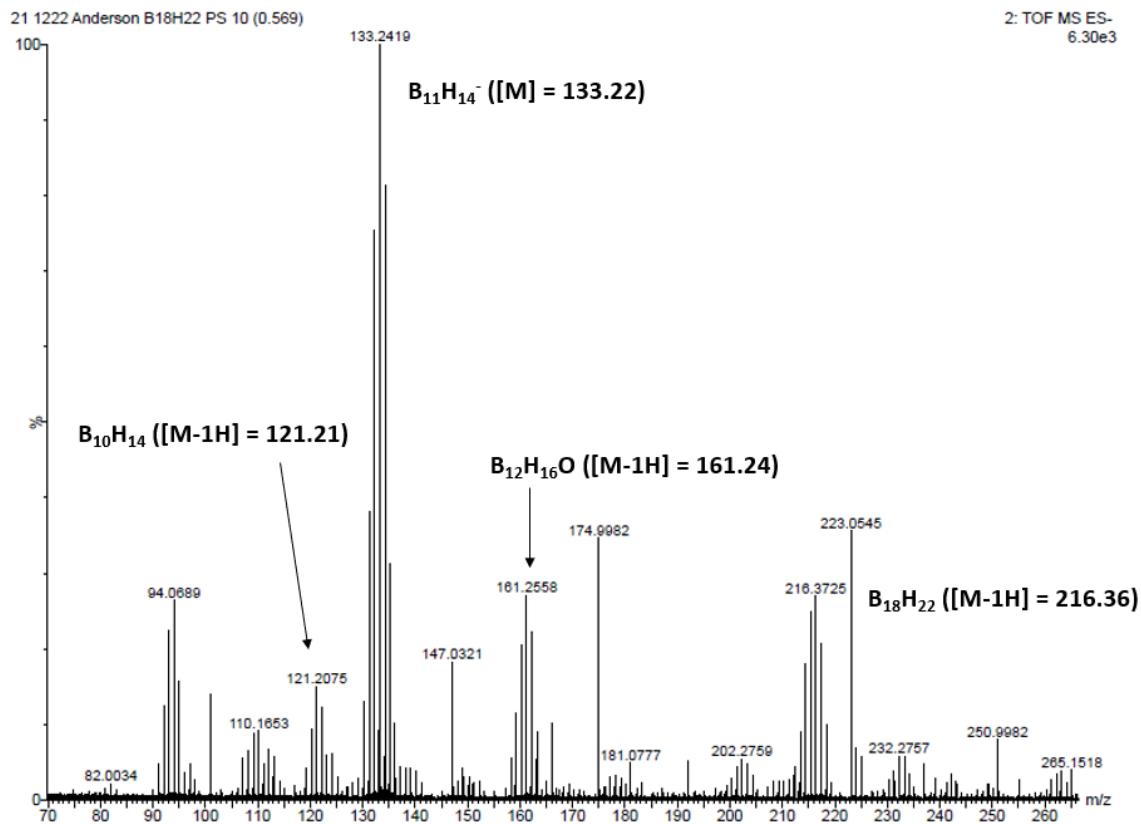


Figure S36. ESI(-) MS of closed vessel PS-1 after 7 days of 266 nm light exposure.

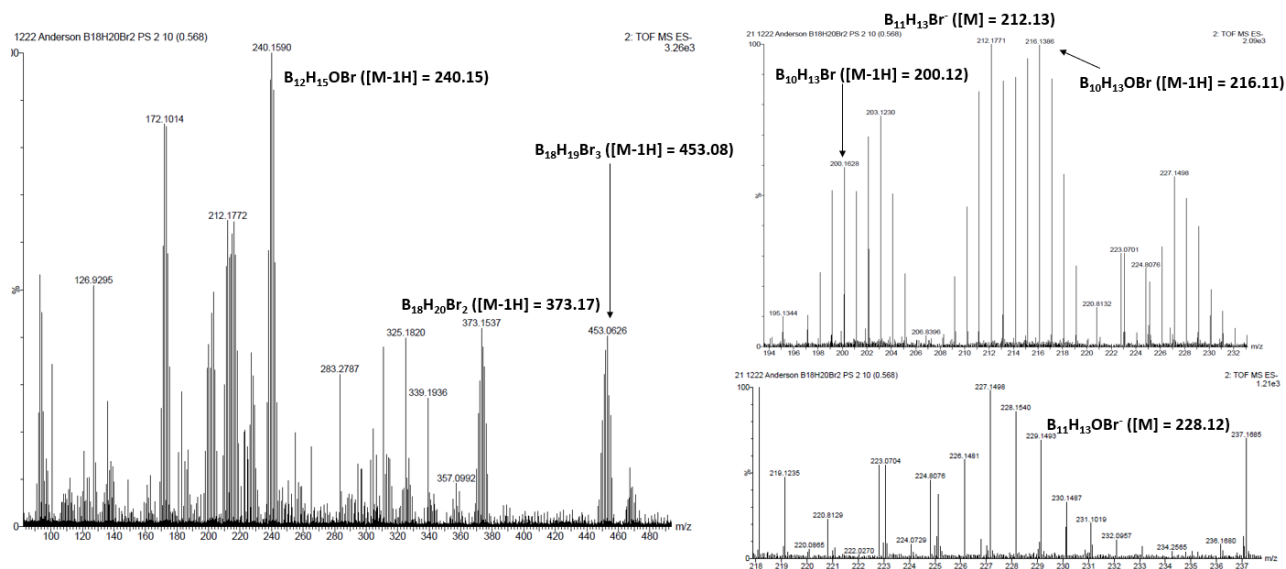
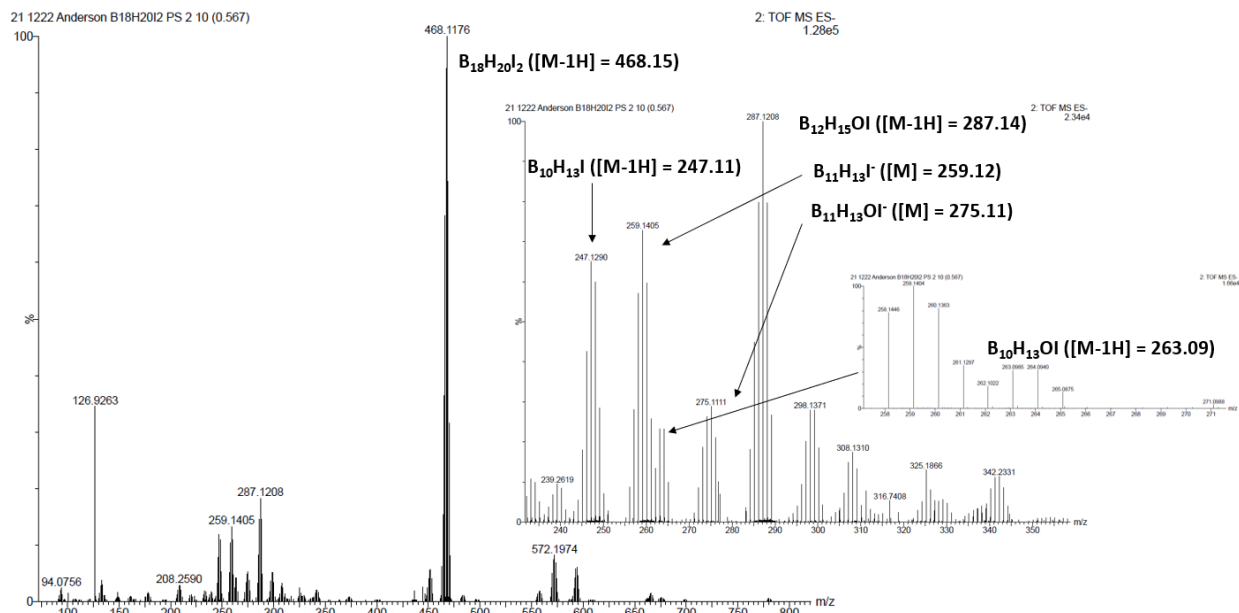
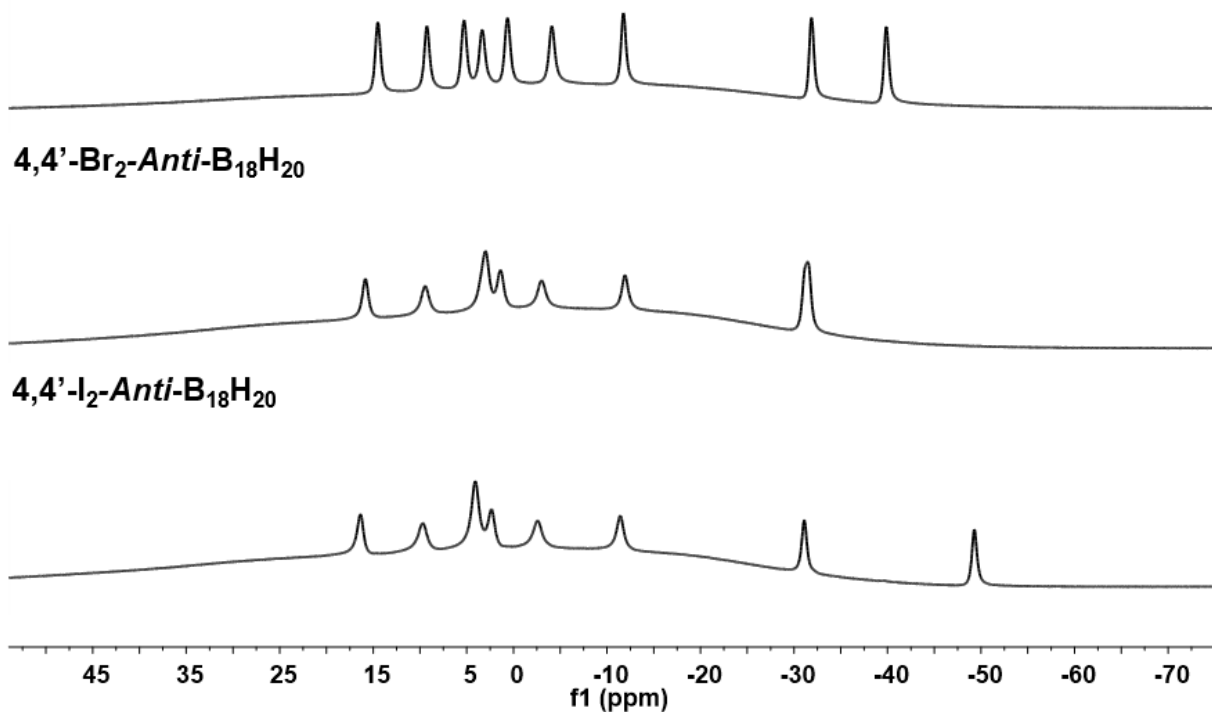


Figure S37. ESI(-) MS of closed vessel PS-2 after 7 days of 266 nm light exposure.



**Figure S38.** ESI(-) MS of closed vessel **PS-3** after 7 days of 266 nm light exposure.

***Anti-B<sub>18</sub>H<sub>22</sub>***



**Figure S39.**  $^{11}\text{B}\{^1\text{H}\}$  NMR spectra of powders **1**, **2** and **3** after 7 days of 266 nm light exposure. The masses of the powders measured before and after irradiation were similar, indicating little to no degradation occurred.

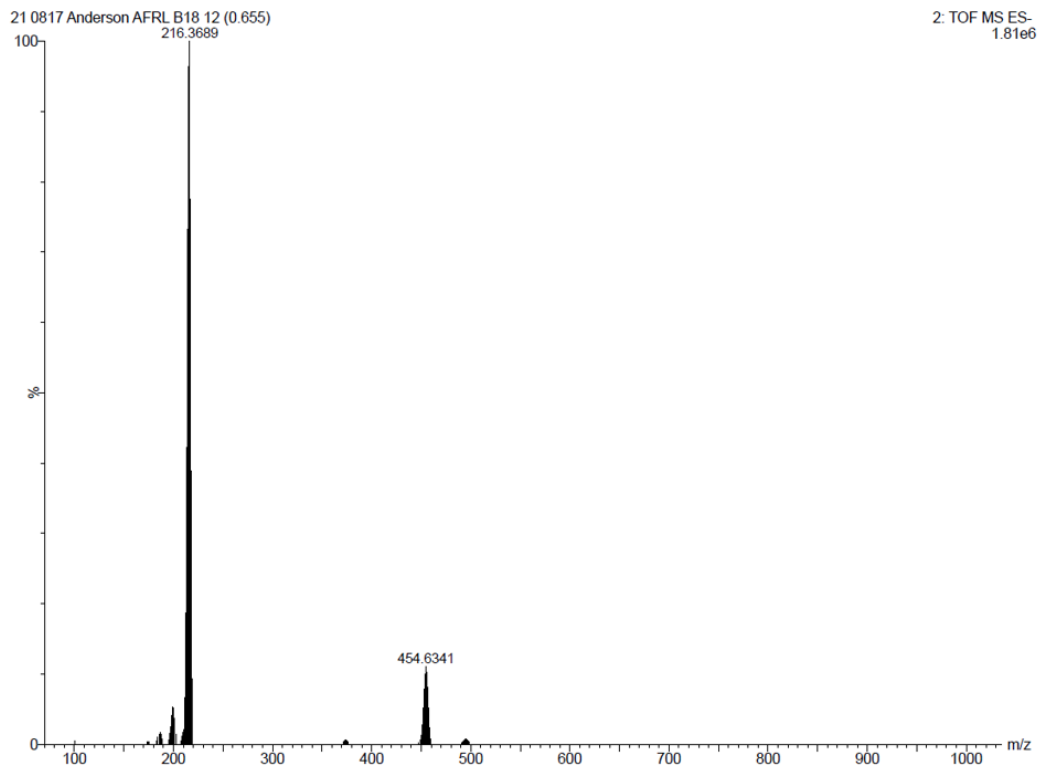


**Figure S40.** ESI(-) MS of powder **1** 7 days of 266 nm light exposure.

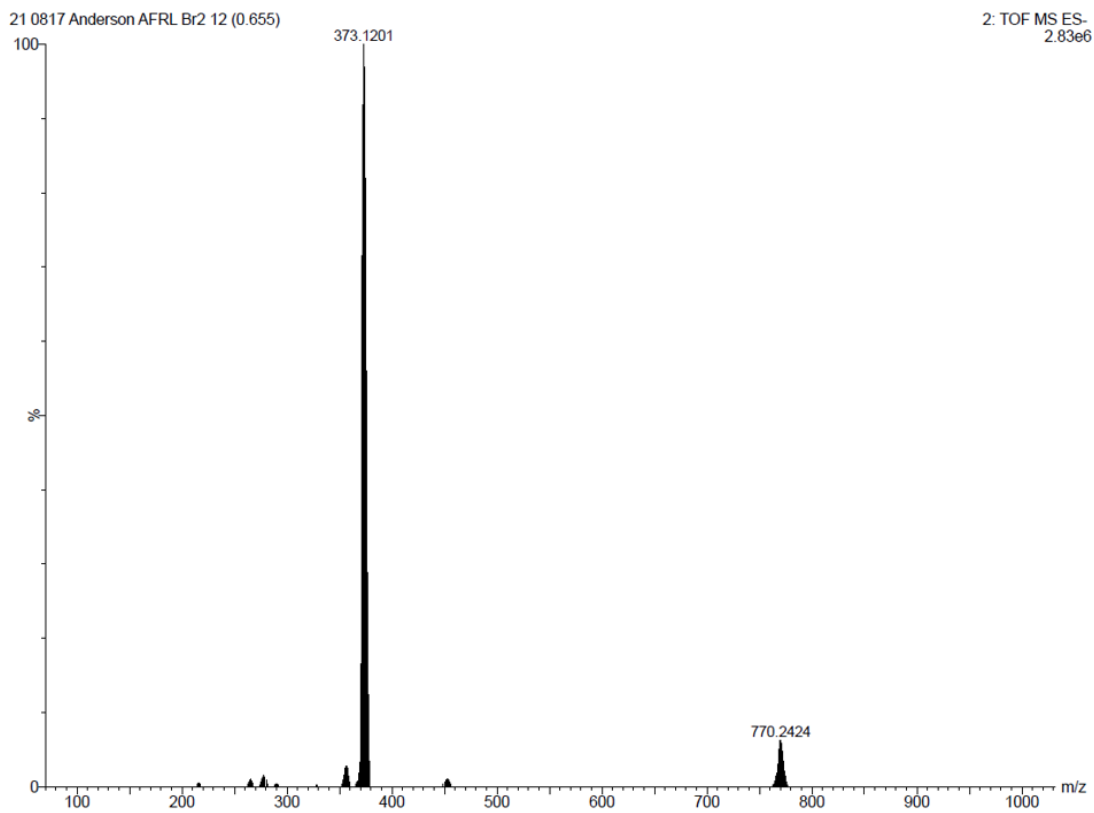


**Figure S41.** ESI(-) MS of powder **2** 7 days of 266 nm light exposure.

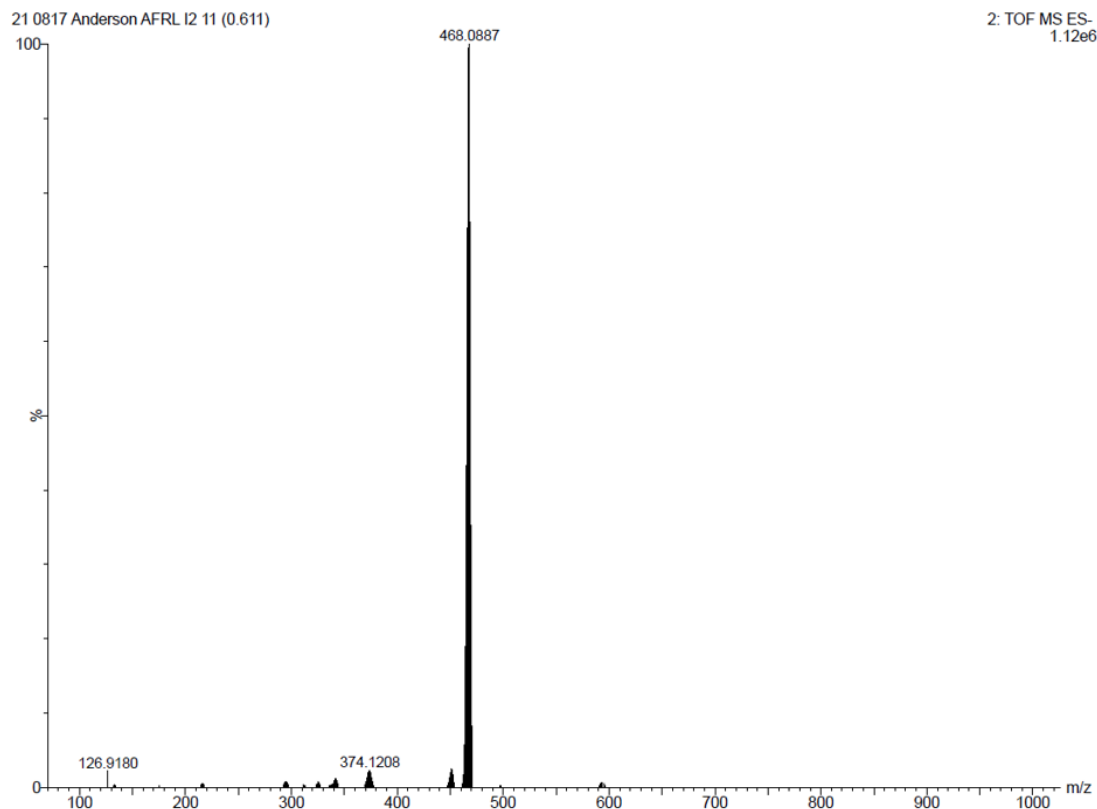


**Figure S42.** ESI(-) MS of powder **3** 7 days of 266 nm light exposure.

## Inductively-Coupled Plasma – Optical Emission Spectroscopy (ICP-OES) Studies

**Preparation of thin films on quartz:** PMMA: 50 mg PMMA was dissolved in 2 mL toluene under ambient conditions. B<sub>18</sub>H<sub>22</sub> (2 mg) was added to give a 2 wt% solution. The solution was spin coated in an even layer onto a clean 1x1 inch quartz substrate using a glass pipet and dried over 24 hrs.

PS: 50 mg polystyrene was dissolved in 1 mL toluene under ambient conditions. B<sub>18</sub>H<sub>22</sub> (1 mg) was added to give a 2 wt% solution. The solution was dropcast in an even layer onto a clean 1x1 inch quartz substrate using a glass pipet and dried over 24 hrs.

**Sample preparation:** Samples were redissolved in scintillation vials by adding ~10 mL dichloromethane and letting stir overnight. They were transferred to 30 mL microwave vials with multiple dichloromethane washes and then evaporated over the weekend prior to acid digestion.

**Sample digestion:**

HNO<sub>3</sub> (Trace Metal Grade) was added to each microwave vial.

- 10 mL HNO<sub>3</sub> for 1 mg cluster (PS films)
- 20 mL HNO<sub>3</sub> for 2 mg cluster (PMMA films)

Samples were digested in a CEM Discover SP Microwave Reactor.

- 100 W, ~10 min ramp, 5 min hold at 175°C for 10 mL volume
- 130 W, ~6.5 min ramp, 5 min hold at 175°C for 20 mL volume

A 1.4 mL aliquot was then transferred to a 14 mL Falcon centrifuge tube and diluted to a total volume of 14.0 mL with HPLC grade water to create solutions of 10% HNO<sub>3</sub>. A gelatinous precipitate was observed to form in some samples, presumably due to the low solubility of the organic films in aqueous solution. Cloudy solutions were filtered through a 0.45 µm syringe filter until clear, multiple times if necessary.

PS and PMMA Controls (no cluster) were used to quantify the amount of boron that leached into solution from the borosilicate microwave vials during digestion.

**Table S3.** Summarized ICP results for PMMA and PS films after irradiation. The percent remaining values were calculated by dividing the measured boron content from the irradiated films by that of the control film (either PS or PMMA) loaded with *anti*-B<sub>18</sub>H<sub>22</sub>.

	PS film (ppm)	Percent remaining	PMMA film (ppm)	Percent remaining
<i>anti</i> -B <sub>18</sub> H <sub>22</sub> (1)	1.27	27%	0.73	47%
4,4'-Br <sub>2</sub> - <i>anti</i> -B <sub>18</sub> H <sub>20</sub> (2)	0.15	3%	0.20	13%
4,4'-I <sub>2</sub> - <i>anti</i> -B <sub>18</sub> H <sub>20</sub> (3)	1.52	32%	0.05	3%

**Table S4.** Complete ICP results for PMMA and PS films after irradiation.

Sample	MW	Cluster (mg)	HNO <sub>3</sub> Digest Volume (mL)	Conc in Digest (mg/ml)	Conc in Digest (M)	Total Soln Volume (mL)	Aliquot (mL)	Conc in Measured Sol'n (M)	Expected B (g)	Expected B (ppm = mg/L)	Measured B (ppm)
B <sub>18</sub> H <sub>22</sub> Control 1 mg	217.35	1.0	10	0.100	4.60E-04	14.0	1.4	4.60087E-05	8.95238E-06	9	7.27
B <sub>18</sub> H <sub>22</sub> Control 2 mg	217.35	2.0	20	0.100	4.60E-04	14.0	1.4	4.60087E-05	8.95238E-06	9	9.88
No B <sub>18</sub> H <sub>22</sub> PS Control			10			14.0	1.4				0.03
No B <sub>18</sub> H <sub>22</sub> PMMA Control			20			14.0	1.4				0.07
B <sub>18</sub> H <sub>22</sub> PS Control	217.35	1.0	10	0.100	4.60E-04	14.0	1.4	4.60087E-05	8.95238E-06	9	4.68
B <sub>18</sub> H <sub>22</sub> PS	217.35	1.0	10	0.100	4.60E-04	14.0	1.4	4.60087E-05	8.95238E-06	9	1.27
B <sub>18</sub> H <sub>22</sub> PMMA Control	217.35	2.0	20	0.100	4.60E-04	14.0	1.4	4.60087E-05	8.95238E-06	9	1.54
B <sub>18</sub> H <sub>22</sub> PMMA	217.35	2.0	20	0.100	4.60E-04	14.0	1.4	4.60087E-05	8.95238E-06	9	0.73
B <sub>18</sub> H <sub>20</sub> Br <sub>2</sub> PS	374.17	1.0	10	0.100	2.67E-04	14.0	1.4	2.67258E-05	5.20031E-06	5	0.15
B <sub>18</sub> H <sub>20</sub> I <sub>2</sub> PS	469.14	1.0	10	0.100	2.13E-04	14.0	1.4	2.13156E-05	4.14759E-06	4	1.52
B <sub>18</sub> H <sub>20</sub> Br <sub>2</sub> PMMA Control	374.17	2.0	20	0.100	2.67E-04	14.0	1.4	2.67258E-05	5.20031E-06	5	0.20
B <sub>18</sub> H <sub>20</sub> I <sub>2</sub> PMMA	469.14	2.0	20	0.100	2.13E-04	14.0	1.4	2.13156E-05	4.14759E-06	4	0.05

## UV Imaging Test

**Preparation of thin films:** To four 5 mL vials, 25 mg of polystyrene and 1 mL toluene was added and sonicated at 40°C for 30 minutes until the polystyrene was fully dissolved. To three vials, 2.5 mg of select emitter (*anti*-B<sub>18</sub>H<sub>22</sub>, 4,4'-Br<sub>2</sub>-*anti*-B<sub>18</sub>H<sub>20</sub>, or 4,4'-I<sub>2</sub>-*anti*-B<sub>18</sub>H<sub>20</sub>) was added. To the fourth vial, 100 mg benzophenone was added. All solutions were sonicated at 40°C for another 5 minutes until dissolved.

UV absorbing patterns were applied to a 1x1 inch quartz substrate using a spotting capillary tube. The emissive films were prepared by casting the polystyrene-emitter solution onto 1x1 inch quartz substrates.

**UV Imaging:** A 340 nm LED was mounted onto a stand and placed behind a 340 nm bandpass filter and focusing lens. The UV absorbing film on quartz was secured on the other side of the bandpass filter with a binder clip. The emissive film was placed directly in front of the UV absorbing film and secured using the same binder clip. Photos were taken with a Pixel 5a camera.

## Calculations

Calculations were performed using SCM ADF software with TD-DFT capabilities. Optimized geometries were calculated using the hybrid PBE0 functional and the DZP basis set with scalar relativistic effects considered. Frequency analysis was carried out to confirm the local minima.

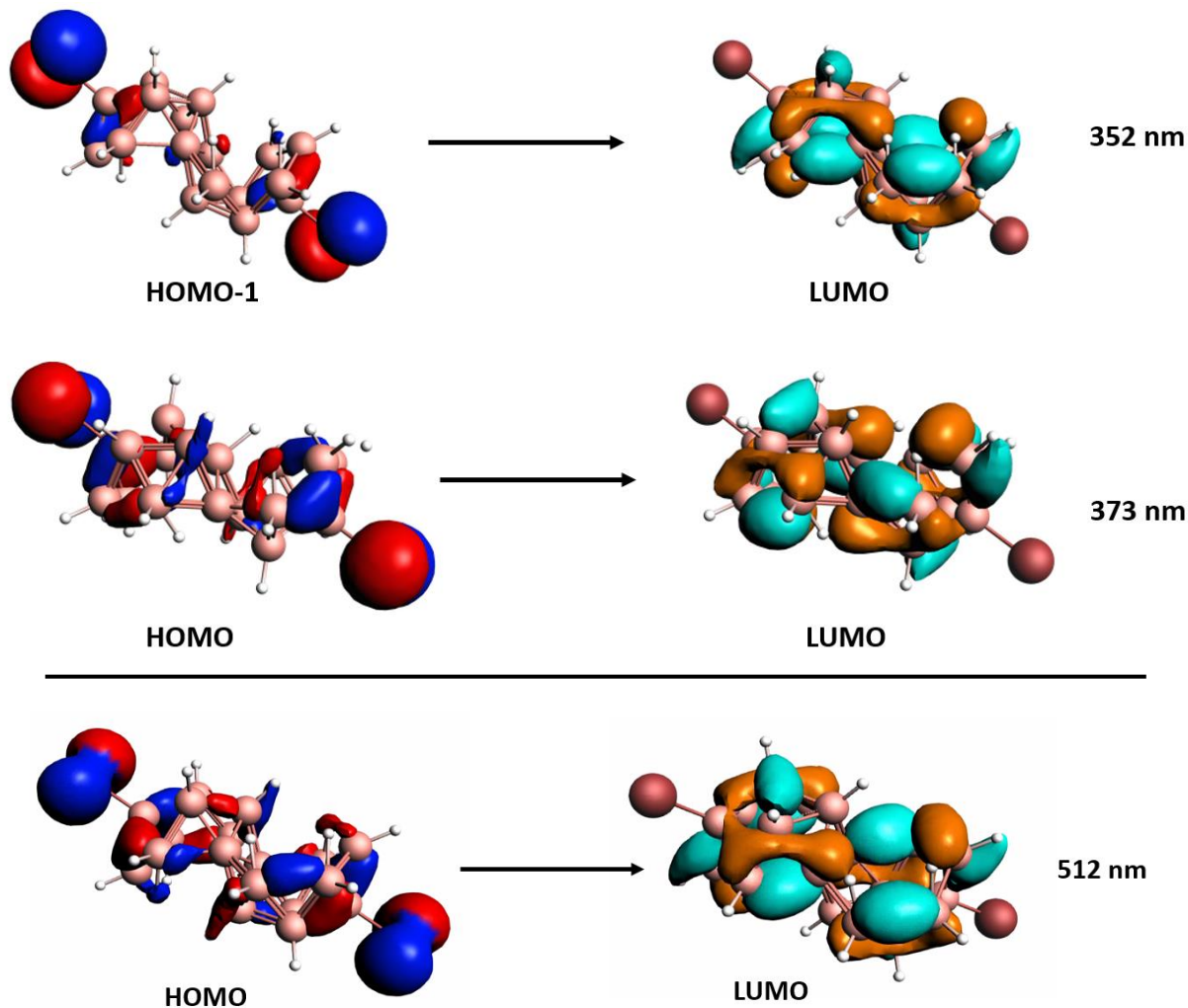


**Figure S43.** Natural Transition Orbitals of the excitation (top) and emission spectra (bottom) of **2**. The excitation spectrum was calculated from the  $S_0$  state optimized geometry. The emission spectrum was calculated from the  $T_1$  optimized geometry. Wavelengths at which these events are observed are listed on the right.

**Table S5.** The PBE0 DZP optimized geometry coordinates for the  $S_0$  state of 4,4'-Br<sub>2</sub>-*anti*-B<sub>18</sub>H<sub>20</sub>.

H	2.40803702	-1.47276003	3.92826748
B	-0.33462758	0.20054952	1.70377732
B	1.54968124	3.28000398	2.55379251
B	-0.21184758	3.31462397	2.22220061
H	-0.85301024	4.30382448	2.11127737
H	-0.70366723	2.66752309	3.25565759
B	0.88646856	2.72550485	1.01069408
B	2.12977772	1.75701713	1.83359284
H	3.27622097	1.65512336	1.54548475

B	1.79569388	1.83097772	3.53767223
H	2.62772970	1.65120547	4.36057852
H	0.64430441	1.68531540	4.15547733
B	0.46364582	2.94747107	3.83263922
H	0.24975930	3.54683242	4.82917404
B	-0.62021069	1.84422561	1.02092779
H	-1.43524394	1.99867765	0.17562777
H	2.18015356	-0.66058731	2.11887989
B	0.92534447	0.99519022	0.78053259
H	1.29989279	0.56669734	-0.26058696
B	1.30879018	0.32473874	2.39884898
H	-0.06148803	-2.89589280	4.04011702
H	1.03296004	3.42226414	0.06248493
B	-0.57408143	-2.75567111	1.54752998
B	1.18622695	-2.79049929	1.88228757
H	1.82753963	-3.77933148	1.99527634
H	1.68034248	-2.14344210	0.84946246
B	0.08629658	-2.19981722	3.09160503
B	-1.15586246	-1.23159082	2.26718797
H	-2.30276233	-1.13084491	2.55402965
B	-0.81866322	-1.30618256	0.56315461
H	-1.64793069	-1.12531828	-0.26228821
H	0.33487208	-1.16007039	-0.05093149
B	0.51400978	-2.42234360	0.27034362
H	0.72877651	-3.02099543	-0.72642749
B	1.59322933	-1.31853991	3.08274758
Br	2.70497066	4.85628974	2.59753213
H	-1.20716546	1.18578178	1.98442763
B	0.04730732	-0.46954078	3.32168746
H	-0.32773682	-0.04037091	4.36229595
Br	-1.72952658	-4.33074210	1.50034290

**Table S6.** The PBE0 DZP optimized geometry coordinates for the T<sub>1</sub> state of 4,4'-Br<sub>2</sub>-*anti*-B<sub>18</sub>H<sub>20</sub>.

H	2.45098167	-1.52080031	3.87638971
B	-0.34070827	0.18159425	1.69541216
B	1.52369537	3.24001809	2.55759259
B	-0.24118512	3.29834034	2.20925518
H	-0.83280511	4.31678950	2.08015124
H	-0.74632993	2.69562693	3.31860952
B	0.89481300	2.70218610	0.97226273
B	2.13734844	1.77897109	1.80639217
H	3.27549401	1.69463697	1.48368519

B	1.74747329	1.72646398	3.52009138
H	2.58424904	1.57254444	4.34518868
H	0.58082111	1.74611284	4.22809959
B	0.41124119	2.95727318	3.84248238
H	0.32916054	3.67388849	4.77993080
B	-0.64212789	1.88667252	1.05305122
H	-1.47675320	2.04660041	0.22651175
H	2.16393693	-0.61491229	2.10155112
B	0.91448498	0.97917306	0.77136958
H	1.34175757	0.53152705	-0.24263974
B	1.31535702	0.34378417	2.40684251
H	-0.08797227	-2.89498184	4.05918388
H	1.06206827	3.42065263	0.04332173
B	-0.54868725	-2.71482568	1.54461386
B	1.21600717	-2.77325683	1.89376534
H	1.80748170	-3.79171756	2.02344889
H	1.72182878	-2.17095739	0.78449408
B	0.07955385	-2.17670364	3.13014608
B	-1.16269827	-1.25372129	2.29531054
H	-2.30097883	-1.16941841	2.61753192
B	-0.77183114	-1.20140795	0.58182843
H	-1.60805746	-1.04752766	-0.24383120
H	0.39532442	-1.22099597	-0.12530793
B	0.56438881	-2.43225729	0.26021069
H	0.64673672	-3.14879668	-0.67727173
B	1.61650831	-1.36113424	3.04965027
Br	2.66143760	4.80957130	2.67155264
H	-1.18951042	1.14005914	2.00084801
B	0.05981334	-0.45366467	3.33072828
H	-0.36763604	-0.00573105	4.34453222
Br	-1.68647523	-4.28437907	1.43039579

**Table S7.** The PBE0 DZP frequency calculations for the S<sub>0</sub> state of 4,4'-Br<sub>2</sub>-*anti*-B<sub>18</sub>H<sub>20</sub>.

A\_1 : 68.1  
A\_2 : 73.0  
A\_3 : 102.1  
A\_4 : 116.3  
A\_5 : 137.5  
A\_6 : 163.2  
A\_7 : 213.4  
A\_8 : 241.3  
A\_9 : 265.3  
A\_10 : 280.2

A\_11 : 316.1  
A\_12 : 348.6  
A\_13 : 405.9  
A\_14 : 406.4  
A\_15 : 419.0  
A\_16 : 430.5  
A\_17 : 472.3  
A\_18 : 475.3  
A\_19 : 490.7  
A\_20 : 533.3  
A\_21 : 560.5  
A\_22 : 561.1  
A\_23 : 581.1  
A\_24 : 588.2  
A\_25 : 599.2  
A\_26 : 609.4  
A\_27 : 620.3  
A\_28 : 625.6  
A\_29 : 637.0  
A\_30 : 644.0  
A\_31 : 653.3  
A\_32 : 661.7  
A\_33 : 671.7  
A\_34 : 675.7  
A\_35 : 689.8  
A\_36 : 693.8  
A\_37 : 706.4  
A\_38 : 717.5  
A\_39 : 720.7  
A\_40 : 725.2  
A\_41 : 732.5  
A\_42 : 736.4  
A\_43 : 744.9  
A\_44 : 747.7  
A\_45 : 755.3  
A\_46 : 771.0  
A\_47 : 772.3  
A\_48 : 774.8  
A\_49 : 791.0  
A\_50 : 791.4  
A\_51 : 801.1  
A\_52 : 806.2  
A\_53 : 815.4  
A\_54 : 817.6  
A\_55 : 823.1  
A\_56 : 827.8

A\_57 : 830.2  
A\_58 : 865.8  
A\_59 : 879.8  
A\_60 : 880.3  
A\_61 : 887.3  
A\_62 : 888.0  
A\_63 : 903.8  
A\_64 : 919.7  
A\_65 : 921.8  
A\_66 : 923.0  
A\_67 : 925.9  
A\_68 : 937.0  
A\_69 : 943.6  
A\_70 : 946.2  
A\_71 : 947.4  
A\_72 : 950.9  
A\_73 : 959.9  
A\_74 : 976.2  
A\_75 : 978.1  
A\_76 : 985.1  
A\_77 : 996.4  
A\_78 : 1000.1  
A\_79 : 1008.6  
A\_80 : 1014.5  
A\_81 : 1018.7  
A\_82 : 1030.1  
A\_83 : 1036.9  
A\_84 : 1043.1  
A\_85 : 1058.8  
A\_86 : 1059.1  
A\_87 : 1100.0  
A\_88 : 1102.5  
A\_89 : 1572.6  
A\_90 : 1578.6  
A\_91 : 1673.5  
A\_92 : 1675.6  
A\_93 : 1719.7  
A\_94 : 1723.3  
A\_95 : 2035.3  
A\_96 : 2036.2  
A\_97 : 2072.7  
A\_98 : 2073.0  
A\_99 : 2097.6  
A\_100 : 2099.9  
A\_101 : 2683.5  
A\_102 : 2683.9

A\_103 : 2692.7  
A\_104 : 2693.0  
A\_105 : 2702.4  
A\_106 : 2702.7  
A\_107 : 2712.2  
A\_108 : 2712.8  
A\_109 : 2718.1  
A\_110 : 2718.3  
A\_111 : 2722.3  
A\_112 : 2722.7  
A\_113 : 2744.1  
A\_114 : 2744.1

**Table S8.** The PBE0 DZP frequency calculations for the T<sub>1</sub> state of 4,4'-Br<sub>2</sub>-*anti*-B<sub>18</sub>H<sub>20</sub>.

A\_1 : 66.4  
A\_2 : 68.6  
A\_3 : 109.3  
A\_4 : 116.5  
A\_5 : 139.8  
A\_6 : 164.3  
A\_7 : 211.4  
A\_8 : 249.2  
A\_9 : 255.3  
A\_10 : 257.4  
A\_11 : 320.9  
A\_12 : 346.2  
A\_13 : 398.4  
A\_14 : 403.6  
A\_15 : 447.6  
A\_16 : 465.6  
A\_17 : 471.7  
A\_18 : 492.2  
A\_19 : 508.0  
A\_20 : 519.6  
A\_21 : 527.7  
A\_22 : 545.2  
A\_23 : 549.5  
A\_24 : 549.8  
A\_25 : 559.3  
A\_26 : 587.3  
A\_27 : 587.5  
A\_28 : 595.0  
A\_29 : 605.1  
A\_30 : 623.0  
A\_31 : 625.0

A\_32 : 640.1  
A\_33 : 651.3  
A\_34 : 664.6  
A\_35 : 676.7  
A\_36 : 687.9  
A\_37 : 692.5  
A\_38 : 699.2  
A\_39 : 707.3  
A\_40 : 709.6  
A\_41 : 714.3  
A\_42 : 714.5  
A\_43 : 720.0  
A\_44 : 724.5  
A\_45 : 738.3  
A\_46 : 741.8  
A\_47 : 747.9  
A\_48 : 755.7  
A\_49 : 765.6  
A\_50 : 772.7  
A\_51 : 788.3  
A\_52 : 790.5  
A\_53 : 795.3  
A\_54 : 797.3  
A\_55 : 800.7  
A\_56 : 811.7  
A\_57 : 812.8  
A\_58 : 842.6  
A\_59 : 846.5  
A\_60 : 859.0  
A\_61 : 866.6  
A\_62 : 871.8  
A\_63 : 878.7  
A\_64 : 882.1  
A\_65 : 901.8  
A\_66 : 904.4  
A\_67 : 908.0  
A\_68 : 909.1  
A\_69 : 910.0  
A\_70 : 918.6  
A\_71 : 922.0  
A\_72 : 928.2  
A\_73 : 928.3  
A\_74 : 947.4  
A\_75 : 951.9  
A\_76 : 958.4  
A\_77 : 966.9

A\_78 : 968.1  
A\_79 : 985.5  
A\_80 : 994.8  
A\_81 : 999.3  
A\_82 : 1002.4  
A\_83 : 1014.0  
A\_84 : 1015.8  
A\_85 : 1045.1  
A\_86 : 1047.9  
A\_87 : 1077.4  
A\_88 : 1081.9  
A\_89 : 1439.9  
A\_90 : 1440.7  
A\_91 : 1576.1  
A\_92 : 1589.6  
A\_93 : 1628.8  
A\_94 : 1636.4  
A\_95 : 2023.7  
A\_96 : 2027.9  
A\_97 : 2079.6  
A\_98 : 2082.7  
A\_99 : 2131.0  
A\_100 : 2132.7  
A\_101 : 2668.9  
A\_102 : 2669.5  
A\_103 : 2694.5  
A\_104 : 2694.6  
A\_105 : 2698.5  
A\_106 : 2698.6  
A\_107 : 2701.4  
A\_108 : 2702.6  
A\_109 : 2707.9  
A\_110 : 2708.4  
A\_111 : 2713.6  
A\_112 : 2713.7  
A\_113 : 2731.6  
A\_114 : 2731.8

## References

1. M. G. S. Londesborough, J. Dolanský, J. Bould, J. Braborec, K. Kirakci, K. Lang, I. Císařová, P. Kubát, D. Roca-Sanjuán, A. Francés-Monerris, L. Slušná, E. Noskovičová and D. Lorenc, *Inorganic Chemistry*, 2019, **58**, 10248-10259.
2. T. Sahlstrom, P. Hausgen, J. Guerrero, A. Howard, and N.A. Snyder. Presented in part at the 33rd IEEE Photovoltaic Specialists Conference, May, 2008.